LBL-24146
Preprint

Lawrence Berkeley Laboratory
UNIVERSITY OF CALIFORNIA

Physics Division

Mathematics Department

Submitted to Journal of Crystal Growth

On Kinetics and Hydrodynamics Related to the Growth of Faceted Crystals

P. Haldenwang

September 1987

Prepared for the U.S. Department of Energy under Contract DE-AC03-76SF00098

DISCLAIMER

ON KINETICS AND HYDRODYNAMICS RELATED TO THE GROWTH OF FACETED CRYSTALS[1]

Pierre Haldenwang[2]

Department of Mathematics
and
Lawrence Berkeley Laboratory
University of California
Berkeley, California 94720

September 1987

Abstract

The aim of this study is to propose a generalized model of crystal growth kinetics. This work is conceived to allow a faceted crystal to grow uniformly in a non-uniform fluid environment. The result appears as a partial differential equation (PDE) whose solution characterizes the surface profile. This P.D.E is intended to be coupled, through interfacial supersaturation and mass flux, with the P.D.Es driving transport and dynamics in the fluid phase.

This paper also comes back to the origin of the morphological instability of faceted crystals and gives new considerations on this purpose. Especially we study the coupling of an uniform growth with two basic laminar fluid flows: Blasius flow and buoyancy layer flow of natural convection. Results concerning the limit size of the crystal face before appearence of morphological instability are given in both cases. Some comments are additionally presented for turbulent flows.

---

[1]Supported in part by the Applied Mathematical Sciences Subprogram of the Office of Energy Research, U.S. Department of Energy under contract DE-AC03-76SF00098.

[2]Present address: Laboratoire de Combustion et Hydrodynamique, Universite de Provence, Centre de Saint-Jerome, 13397 Marseille Cedex 13, France.

I.] Introduction

A special feature of faceted crystal is to be able to grow uniformly despite a non-uniform fluid environment. But this property fails in many experiments as soon as a certain limit of nonuniformity is reached. This limit can be either a critical growth rate or a too large size of the crystal. A morphological instability is then observed as largely reviewed in [1-3]. This is the result of a disadvantageous coupling between the crystal kinetics and the transport processes in the fluid phase. On the other hand, a stable growth is also the result of a coupled process: the crystal extracts from the fluid phase a uniform mass flux permitted by the transport processes.

To predict such a phenomenon in a general manner one needs to go a little bit further the classical models of crystal kinetics. The usual formulae give the growth rate with respect to a global supersaturation (its value in the bulk). This corresponds to an attempt to already take into account the transport in the fluid volume. In this cases, the transport in the fluid phase is limited to the diffusion in a thin fluid layer supposed at rest. The coupling between the crystal kinetics and the fluid phase transport can be analytically carried out [4,5]. But in most of the cases, fluid at rest cannot be assumed.

First, we need a microscopic model that relates the crystal kinetics to the supersaturation directly at the interface. In such way we would have on one side, the modelization of Fluid Mechanics and on the other one, an intrinsic behaviour of a crystal in contact with a fluid phase. For that purpose the Burton-Cabrera-Frank model [6] seems to be advantageous, although controverted for the growth from liquid phase. Moreover, as it will be reminded in Part.II, this model leads to a convincing interpretation of the morphological instability of faceted crystals grown from solution. This part is also the opportunity to discuss the criterion of Kuroda, Irisawa and Ookawa [7] for the growth stability of faceted crystals.

The use of this criterion allows us to derive severe consequences for the stability of faceted crystals grown in presence of two basic fluid flows. This is carried out in Part.III. Any experimental confirmation of those results would, by the way, reinforce the idea according to which the same growth model is available for both fluid phases.

In Part.IV we present the model of generalized kinetics. The latter appears as a two-dimensional Partial Differential Equation (PDE) that one has to couple with the PDE system governing the fluid phase. We give several illustrations of the results that can be obtained by resolving this PDE in various cases including unstable growth, unsteady environment or anisotropic growth. Moreover we believe this model is continuously applicable from faceted growth to the non-faceted one.

II.] Step propagation and stability criterion.

There is a general agreement for stating a crystal grows thanks to the propagation of steps along preferred crystal faces. The term "step" means either an elementary lattice layer or a macro-step (or waves) obtained after some bunching process of the former ones. The authors however differ in view of the step propagation velocity. The latter point is crucial because faceted crystals exist only because step propagation is faster than step generation.

Among the numerous models of propagation velocity of steps (see e.g. [1,3]), we first eliminate those that state the step propagation is controlled by volume diffusion in the fluid. In fact, those models are attempts to already take into account the coupling with a surrounding immobile fluid layer (if any). However surface diffusion of adsorbed components is more pleasant for our purpose. This corresponds to an intrinsic mechanism of the crystal kinetics because it does not involve any transport process in the fluid phase. Although this mechanism was originally recognized as the controlling process for growth in vapor phase, the classical model [6] of Burton, Cabrera and Frank (BCF) have received some experimental confirmation in growth from liquid phase [8].

In the BCF model of step propagation the role played by adsorbed components diffusing along the interface, is supposed to be dominant in the constitution of the step ledge. So the step velocity reads:

$$V_{st} = K_{st}\,\sigma\,[\tanh\frac{(x_{n+1}-x_n)}{2\lambda_s} + \tanh\frac{(x_n-x_{n-1})}{2\lambda_s}] \qquad (1)$$

where σ is the supersaturation at the fluid-crystal interface and λ_s is the characteristic diffusion length of the adsorbed particles. The position of the step of order n is x_n. For the origin of K_{st}, the kinetic coefficient the reader is invited to refer to the BCF original paper (1951).

In addition to theoretical basements, such a model contains convincing behaviours : the step velocity tends to a finite limit when the crystal profile becomes infinitely flat ($[x_{n+1}-x_n]>>2\lambda_s$) (Property P.1). and becomes proportional to the interstep distance when those are in competition (Property P.2). With such a velocity model, an infinite train of equally spaced steps can propagate with a constant profile in a uniform supersaturation. But if the train is finite the leading step having a larger velocity will stretch the global pattern. A crystal face whose the interstep distance indefinitely increases will become more and more flat.

But from experimental considerations a step train can also stop (see e.g. [9]) leading to discontinuities that can heal, giving liquid phase inclusions or veils. For a long time the reasons of this train stop were not clear. One early hypothesis, proposed by Carlson [10], was the supersaturation can vanish when the fluid flow passes along a growing surface. And obviously the steps no longer propagate in an exhausted environment. More recently Jansenn-van Rosmalen and Bennema [11]

have reported a complete exhaustion is not necessary to stop a step train. They showed that a sharp discontinuity of the supersaturation along the interface is able to halt a step train driven by Eq.(1). Finally both explanations are contained in the more general interpretation of Kuroda, Irisawa and Ookawa [7]. Their study concerns equally spaced steps at the microscopic level whose interstep distance $\lambda(x)$ is however supposed to be, at the macroscopic level, a slowly varying function of the local position x. It is then easy to show that the local growth rate is given by :

$$R(x) = \frac{a}{\lambda(x)} V_{st}(x) = \sigma(x) \frac{2a K_{st}}{\lambda(x)} \tanh \frac{\lambda(x)}{2\lambda_s} \tag{2}$$

where a is the height of the steps. Eq.(2) can be rewritten as

$$R(x) = K_R \, \sigma(x) \, G(x) \tag{3}$$

$$\textit{with} \quad K_R = \frac{a K_{st}}{\lambda_s} \tag{4}$$

$$\text{and} \quad G(x) = \frac{2\lambda_s}{\lambda(x)} \tanh \frac{\lambda(x)}{2\lambda_s} \tag{5}$$

The form of the function $G(z)=z^{-1}\tanh(z)$ is given on Fig.1. A decisive argument is developed by the authors as follows. Suppose for some reason in x_0, where the supersaturation is σ_0, the steps are generated with an interstep distance λ_0. So this kinetics is characterized on Fig.1 by the point $\{z_0=\lambda_0/2\lambda_s,\ G_0=G(z_0)\}$. Let us additionally assume there exists along the surface a point where the supersaturation is less than $G_0\sigma_0$. Then considering the form of the curve $G(z)$, one must conclude the step kinetics is no longer able to assure an uniform growth in the latter point.

Such mechanism is very convincing and receives support from two works in which Hydrodynamics is carefully studied. Kumar, Estrin and Youngquist [12] have studied a flow of forced convection coupled with crystal growth. More recently Simon, Cherel and Haldenwang [13] have studied the coupling of crystal growth and the natural convection induced by the growth itself. In the latter work it is shown that the morphological instability, experimentally observed, is caused by gentle depletion of the supersaturation along the crystals.

When the interface is unstable, a discontinuity appears along the surface. The interstep distance sharply varies near the shock and the step density grows indefinitely. So that at the microscopic level an equally spaced distribution of steps is hardly satisfied and Eq.(2) must be subject to question. We have however carried out a numerical study of the dynamics related to Eq.(1) which confirms Eq.(2) persists and the stability criterion remains valid as soon as enough steps are present in the train. This numerical simulation is so simple that we present it just for illustrating the criterion with the following example.

In order to study the effect of a supersaturation drop on the interface stability, we have considered short step trains propagating in contact with a piecewise linear $\sigma(x)$-profile defined on Fig.2. Three equal zones are delimited by x_0=0, x_1=25, x_2=50 and x_{max}=75. The first and last segments have

uniform supersaturations, respectively σ_0 and $\sigma_0(1-d)$. On Fig.2 σ_0 and d are respectively equal to 1 and 0.2 They are connected by the second zone having a linear depletion.

Suppose the steps are generated at x_0 and travel toward x_{max} with a velocity given by Eq.(1). The quantities K_{st} and λ_s are chosen equal to 1. In x_0 we create a new step as soon as the previous one is at a distance larger than λ_0 having a fixed value equal to 1. Then the steps accelerate and reach an average interstep distance in the first uniform supersaturation zone. This value depends on the global supersaturation distribution as shown in what follows.

- For a weak drop of supersaturation (d=0.2) an initially perturbed train rapidly leads to a steady interface profile (see Fig.3a) and a stable growth is obtained. The mean interstep distance is equal to about 5 before the drop of supersaturation and stabilizes around a value of 3.8 after the drop. Although the interstep distances are never equal in this computation, they follows a smooth variation as shown by the Fig.3b where the step density ($=1/\lambda(x)$) is represented. Moreover we verify the interstep distances before and after the drop lead to two values of the function G of which ratio is about 1.27, close to 1.25, the expected value if ones applies the criterion: $R(x)$ is uniform along the face.

- However when d, the drop of supersaturation, passes a critical value the step train no longer propagates and no steady state exists. A discontinuity is created by an unlimited accumulation of steps near the point where the supersaturation approximately corresponds to $G_0\sigma_0$. This expresses the fact that the left part grows with a larger rate than the right one. Interface profiles and step density distributions are presented on Fig.4a and Fig.4b after $1.6\ 10^5$ time units. On Fig4a-b d equals 0.25 and the interstep distance before the drop is 1.9. This gives 0.77 for the value of G that is indeed larger than 0.75, the expected limiting value owing to the criterion.

On Fig.3a and Fig.4a the ordinate gives the number of involved steps. The step density given on Fig.4b is obtained after averaging on five neighbor interstep distances because a crude inverse of the interstep distance would give at certain points singular values.

We conclude this numerical study by considering as reliable the criterion given by Eq.(3), as soon as enough steps are involved in the train. Because this criterion has received some experimental confirmation there is, by the way, a certain[‡] validation of Eq.(1) which is on its basis.

Before leaving this paragraph let us give a quantitative value to the critical drop of supersaturation. If we consider the Fig.1, the larger is the interstep distance around x_0, the more stable is the growth. But from a microscopic point of view the interstep distance cannot increase indefinitely because around x_0 this quantity is fixed by the process of step generation. Following again a BCF model, we can state:

[‡] As a matter of fact we voluntary moderate this statement because, instead Eq.(1), any step velocity formula satisfying the properties P.1 and P.2 would lead to a criterion not very different.

$$\frac{\lambda_0}{2\lambda_\sigma} = \frac{\sigma_1}{\sigma_0} \tag{6}$$

where σ_1 characterizes the crystal face and depends on state variables (temperature, pressure..., cf. the BCF original article). Suppose now we have along the surface an interfacial supersaturation profile whose maximum is σ_{max} and of which minimum is σ_{min}. Furthermore assume x_{max} is a center of step generation. Then the growth will remain stable if the following holds:

$$\frac{\sigma_{min}}{\sigma_{max}} < \frac{\sigma_{max}}{\sigma_1} \tanh\frac{\sigma_1}{\sigma_{max}} \tag{7}$$

The right hand side of this inequality is called the Wilson-Frenkel number [14]. Defining A_σ as the allowed reduced drop of supersaturation, we have:

$$A_\sigma = \frac{\sigma_{max}-\sigma_{min}}{\sigma_{max}} = \begin{bmatrix} 1 & \text{at low supersaturation} \\ \frac{1}{3}\left(\frac{\sigma_1}{\sigma_{max}}\right)^2 & \text{at large supersaturation} \end{bmatrix} \tag{8}$$

Eq.(8) provides an immediate explanation why high growth rate (i.e. high supersaturation) appears as destabilization factor.

Let us now attack simple couplings with Hydrodynamics to study the stability limits of a crystal surface grown in two typical environments of Fluid Mechanics

III.] Morphological Instability and Hydrodynamics

In this part we study the influence of two basic flows on the stability of the growing interface of a faceted crystal. Both flows are commonly encountered in the experimental literature. The first one is a forced flow passing along the crystal surface, while the second one is a flow of natural convection generated along the interface by the growth itself.

All results obtained in this part will be carried out by a crude treatment of the governing equations and the final estimates will relate orders of magnitude and have to be considered as guide for further analysis. Both studies present the same characteristics : first uniform growth is assumed along the surface, then the longitudinal supersaturation profile is estimated, finally we applied the previous stability criterion. We present the results as a limit size of the growing surface, which depends on "external" parameters as bulk supersaturation, growth rate, gravity or flow velocity. The second problem -the natural convection case- is more sensitive than the first one because the flow is induced by the crystal growth itself.

The starting point of this studies are the steady Navier-Stokes equations in the Prandtl boundary layer assumption (See e.g. [15]):

$$(2\text{–}D\ Prandtl\ Eq.) \qquad \left[\begin{array}{c} (u_\perp.\nabla_\perp)\,u_{/\!/} + (u_{/\!/}.\nabla_{/\!/})\,u_{/\!/} = -\nabla_{/\!/} p + \nu\,\nabla_\perp^2 u_{/\!/} \\ \nabla_\perp p = 0 \\ \nabla_{/\!/}.u_{/\!/} + \nabla_\perp.u_\perp = 0 \end{array}\right] \tag{9}$$

where the subscript $/\!/$ (resp. $\perp$) expresses the direction parallel (resp. perpendicular) to the crystal surface ; u and p are the velocity and pressure fields ; ν is the kinematic viscosity.

Let us consider now the conservation equation about σ, the supersaturation. We suppose the latter caused by a component whose mass diffusivity in the fluid is D :

$$(u_\perp.\nabla_\perp)\,\sigma + (u_{/\!/}.\nabla_{/\!/})\,\sigma = D\ \nabla_\perp^2 \sigma \tag{10}$$

We are now concerned with the derivation of relationships between orders of magnitude. Let us define the quantities δ_u, δ_σ, U_σ and l as being the characteristic values of respectively the thickness of the viscous boundary layer, the thickness of the supersaturation boundary layer, the typical value of the parallel velocity in the latter layer and the length of the crystal face in the direction of the flow.

From Eq.(10) it is easy to show (See e.g. [16]) that mass transport balance in the σ-boundary layer gives the following estimate:

$$U_\sigma \frac{\sigma}{l} \approx D \frac{\sigma}{\delta_\sigma^2} \tag{11}$$

At this point let us introduce the flows we are interested on.

III.a] The Blasius flow

The flow entering in contact with a surface parallelly to the latter is one of the most classical flows of the Fluid Mechanics literature. So the following estimates are usual derivations from the Prandtl equations. We have first to define U_∞ as the velocity parallel to the crystal at large distance of it. This quantity is a directly tunable experimental parameter. In the Blasius flow it is well established (See for instance [17]) that the viscous boundary layer thickness increases as the square root of the distance from the leading edge. So that we have typically:

$$\delta_u \approx \left[\frac{l\nu}{U_\infty}\right]^{1/2} \tag{12}$$

Accordingly to a linear profile of the viscous boundary layer, we have the following relationship:

$$U_\sigma \approx min\left[\frac{\delta_\sigma}{\delta_u}, 1\right] U_\infty \tag{13}$$

Hence from Eq.(11)-(13) we obtain:

$$\frac{\delta_u}{\delta_\sigma} \approx min\left[S_c^{\frac{1}{3}}, S_c^{\frac{1}{2}}\right] \tag{14}$$

Let us now define $\Delta\sigma = \sigma_0 - \sigma(l)$ as being the longitudinal drop of supersaturation at distance l from the edge. We assume now the growing interface is stable or R, the crystal growth rate is constant along the interface. As the growth rate is related to the mass flux (see e.g. [18]), we have a fixed uniform value of $\nabla_\perp\sigma$, the transverse supersaturation gradient, along the interface. We can then perform a partial integration of Eq.(10) in the direction parallel to the interface and obtain:

$$\Delta\sigma \approx 2 max\left[S_c^{\frac{1}{6}}, 1\right]\left[\frac{D\,l}{U_\infty}\right]^{1/2} \nabla_\perp\sigma \tag{15}$$

It just remains now to apply the criterion exposed in the previous part: there is a critical ratio $A_\sigma = \frac{\sigma_0 - \sigma_{min}}{\sigma_0}$ above which the morphological instability occurs So that Eq.(15) gives l_{max}, the limit

size of stable growth:

$$l_{max} \simeq U_\infty D^{-1} \left[\frac{\sigma_0}{2 \nabla_\perp \sigma} \frac{A_\sigma}{2} \right]^2 \min[S_c^{\frac{-1}{3}}, 1] \qquad (16)$$

To recover the Carlson's results, obtained by application of the starvation principle, it is sufficient to choose $AS=1$ and large Schmidt number in Eq.(16).

If we consider the crystal kinetics of BCF type (quadratic at low supersaturation and linear when the latter is large) we can state the following dependences of l_{max} versus the external parameters:

l_{max} is proportional to $\frac{U_\infty}{\sigma_0^2}$ when σ is low,

l_{max} is proportional to $\frac{U_\infty}{\sigma_0^4}$ at large supersaturation.

For any experimental verification of such dependence it is worth noting that the growth cell have to be maintained at constant temperature. Moreover we believe the previous dependencies are applicable to qualitatively interpret many forced convection flows.

III.b] The buoyancy layer

In a previous work [13], it has been shown the hypothesis of viscous buoyancy layer gives excellent predictions for the flow induced by crystal growth from solution. Let us consider a growing crystal face that is stable. A uniform growth rate requires that a fixed uniform supersaturation gradient is imposed to the solution. Such a concentration gradient produces a mass default along the interface so that a buoyancy force is applied to the fluid in the concentration boundary layer. This force appears as a source term in the right hand side of momentum equations in Eq.(9). The assumption of the viscous buoyancy layer states that the latter force is balanced by the viscous effects so that we have:

$$\nu \frac{U_\sigma}{\delta_\sigma^2} \simeq \gamma g \cos\theta \, \delta_\sigma \nabla_\perp \sigma \qquad (17)$$

where γ is the density variation coefficient, $\gamma=\rho^{-1}(\partial\rho/\partial\sigma)$; $g\cos\theta$ is the projection of $\vec{g}$, the gravity acceleration, on the crystal face. In order to preserve the existence of the buoyancy layer flow we need to assume a moderate value for θ (Say 45°). Then combining Eq.(11) and Eq.(17) we obtain the following estimate:

$$\delta_\sigma \simeq \left[\frac{\nu D \, l}{g \cos\theta \, \gamma \nabla_\perp \sigma} \right]^{\frac{1}{5}} \qquad (18)$$

Likewise in the previous paragraph we evaluate the drop of supersaturation along the interface by partially integrating Eq.(10) in which we suppose $\nabla_\perp \sigma$ is a constant.

$$\Delta\sigma = \sigma_0 - \sigma(l) \approx 5 l^{\frac{1}{5}} (\nabla_\perp \sigma)^{\frac{4}{5}} \left[\frac{\nu D}{g \cos\theta \gamma} \right]^{\frac{1}{5}} \tag{19}$$

Here again we apply the stability criterion by introducing A_σ the critical value for the quantity $1-\sigma_{min}/\sigma_0$. So that the critical length appears as:

$$l_{max} = g \cos\theta \frac{\sigma_0^5}{\nabla_\perp \sigma^4} \left[\frac{A_\sigma}{5} \right]^5 \frac{\gamma}{\nu D} \tag{20}$$

If we again consider a crystal kinetics of BCF type, the dependence of the critical length on the external parameters is the following:

** l_{max} is proportional to $\frac{g \cos\theta}{\sigma_0^3}$ when σ is low

** l_{max} is proportional to $\frac{g \cos\theta}{\sigma_0^9}$ when σ is large.

If we compare such dependence with those obtained with the Blasius flow we notice the gravity here plays the same role than the outer velocity in the latter flow. Recourse to centrifugation, as in [19], has already been used to improve crystal quality. Moreover, if we compare the behaviours of l_{max} at low and high supersaturation, we remark the domain of intermediate supersaturations should correspond to a zone of sharp transition: one goes from an exponent -3 to an exponent -9. So that some value of intermediate supersaturation could experimentally appear as a limit for having clear faceted crystal. The only way to increase the growth rate without distroying the crystal quality is then to increase the gravity.

But at low growth rate the Rayleigh number is generally low and the buoyancy layer assumption is rarely satisfied: our conclusion at low supersaturation have to be tempered. Furthermore, all those results suppose the flow regime is laminar. Fortunately the transition to turbulence can sweeten the tough consequences of Eq.(16) and Eq.(20).

III.c] Turbulent flow

Both precedent flows are known to be subject to transition to turbulence beyond some critical length. Past this point the boundary layer becomes unstable versus sinusoidal perturbations propagating parallelly to the crystal surface. As a result an anomalous mass transport appears transversally to the boundary layer. Hence above l_{cr}, a critical distance, the supersaturation ceases to decay along the interface. This effect clearly appears in the above mentioned work [13] on natural

convection. Likewise the turbulence of the Blasius flow should rapidly stop the drop of supersaturation when the Schmidt number is small or moderate. For larger S_c, the σ-boundary layer being smaller than the viscous one, one needs larger critical length in order that the turbulence affects the transport in the sub-layer. Thus we can state as follows:

> If the system were such that: $l_{cr} < l_{max}$
> then the turbulence would suppress the morphological stability.

* For the Blasius flow, the critical length is known as being related to some critical Reynolds number ($R_{cr}=l_{cr}U_\infty/\nu$): Reporting the value of l_{max} from Eq.(16) we obtain the following condition in order that turbulence allows perfect large crystals.

$$U_\infty^2 \geq R_{cr}(S_c)\left[\frac{\nabla_\perp\sigma}{\sigma_0}\frac{2}{A_\sigma}\right]^2 \nu D\, S_c^{\frac{1}{6}} \tag{21}$$

The critical Reynolds number, as said above, have to be an increasing function of the Schmidt number. In order to give a quantitative sense to inequality (21) we can consider the following typical value: $R_{cr}\approx 10^4$.

* For the buoyancy layer flow the critical length is related to some critical Rayleigh number defined as follows:

$$Ra_{cr} = l_{cr}^4\, \nabla_\perp\sigma\, \frac{g\,\gamma}{D\,\nu} \tag{22}$$

Then combining Eq.(20) and Eq.(22), the fact that l_{cr} is reached before l_{max} is satisfied when the following inequality holds:

$$g^{\frac{5}{4}} \geq Ra_{cr}^{\frac{1}{4}}\, \frac{\nabla_\perp\sigma^{\frac{15}{4}}}{\sigma_0^5}\left[\frac{5}{A_\sigma}\right]^5\left[\frac{\nu D}{\gamma\cos\theta}\right]^{\frac{5}{4}} \tag{23}$$

This inequality well underlines the role that can be played by an ultra-centrifugation set-up to stabilize the growth of a crystal. From a quantitative point of view we need to give a value to Ra_{cr} which is usually a slowly varying function of Sc. Typical values are $Ra_{cr}\approx 10^{10}$.

IV.] A Generalized Kinetics

This part is devoted to expose a generalized model of kinetics allowing to predict the stability of faceted crystal grown in complex fluid environment. This model is applicable to couple 3-D flow with 2-D growing interfaces. This kinetics is also significant with an unsteady flow. We will obtain a time-dependent 2-D partial differential equation that is intended to be simultaneously solved with the time-dependent 3-D Navier-Stokes equations. Such a numerical simulation must recourse to the largest present computing facilities. Results however obtained with the 1-D version of the model coupled with a 2-D hydrodynamics are more accessible and remain significant.

This model starts from the following hypotheses:

On the crystal surface there is zones of step generations, for instance localized on screw dislocations. From these centers start steps or macro-steps having a propagation velocity given by the BCF law [see Eq.(1)]. The zones of step generation enter into rivalry in such way that a generation center can disappear if the latter is overwhelmed by steps issued from more active areas. This happens when step propagation is at this point larger than the step generation. So that only the points, where the step propagation is smaller than the step generation, are candidates for a status as a step generation center.

Let us now consider $S(x,y,t)$, a function depending on the time and the crystal surface space co-ordinates. At a given instant $S(x,y)$ is the sum of the elementary heights of all steps having covered the point (x,y) or born at this point. $S(x,y,t)$ is nothing but the surface state of the growing face. A smooth function S will characterize a crystal having a stable growth. If we define a as the elementary height of a step (or macro-step), then the step profiles correspond to the set of level curves of function $S(x,y,t)$, separated by height a. Moreover the interstep distance is given by:

$$\lambda(x,y) = \frac{a}{|\bar{\nabla}S|} \tag{24}$$

where $\bar{\nabla}S$ is the gradient: $(\frac{\partial S}{\partial x}, \frac{\partial S}{\partial y})$. Let us suppose now the steps propagate normally to itself, i.e. normally to level curves of S. So that the continuous 2-D form of Eq.(1) reads:

$$\bar{V}_{st} = K_{st}\,\sigma\,2\tanh\left[\frac{p_{st}}{|\bar{\nabla}S|}\right]\frac{-\bar{\nabla}S}{|\bar{\nabla}S|} \tag{25}$$

where $p_{st}=\frac{a}{2\lambda_s}$ plays the role of a typical slope controlling the longitudinal propagation. Let us remind σ is the interfacial supersaturation. This quantity is actually the principal unknow of the problem. To determine it we need to couple Eq.(10) (at least) with the final equation of the present study.

As for the growth rate, it is nothing but the time partial derivative of S. It is then easily shown the 2-D continuous version of Eq.(2) takes the form:

$$\left[\frac{\partial S}{\partial t}\right]_{st} = -\bar{\nabla}S \,.\, \bar{V}_{st} = \sigma(x,y)\, K_p\, \frac{|\bar{\nabla}S|}{p_{st}} \tanh\left[\frac{p_{st}}{|\bar{\nabla}S|}\right] \tag{26}$$

where $K_p=2K_s\,p_{st}$. In Eq.(26) the left hand side represents the growth rate resulting from step propagation. By the way let us remind the kinetic constants K_p and p_{st} can eventually depend on (x,y) through the temperature field.

Concerning the growth produced by step generation, only the step creation centers are allowed to have such a contribution. According to our initial assumptions a step creation center must have a feeble growth rate caused by step propagation. Considering Eq.(26) those points are such that $|\bar{\nabla}S|$ is small. Hence the generation centers correspond to the extrema of S. But on the other hand the interstep distance cannot tend to infinity because, if (x,y) is a step generation center, we have at this point a growth rate controlled by Thermodynamics and geometrical properties of the microscopic process. As we have supposed the step creation caused by screw dislocations we can report accordingly to the BCF model:

$$\left[\frac{\partial S}{\partial t}\right]_{g} = K_g\, \frac{\sigma^2(x,y)}{\sigma_1} \tanh\left[\frac{\sigma_1}{\sigma(x,y)}\right] \tag{27}$$

where σ_1 and K_g are kinetic constants which can also depend on (x,y) through the temperature field.

We can now state the creation points are those at which the quantity given by Eq.(27) is larger than the one given by Eq.(26). We finally summerize this property by writing the growth rate at point (x,y), whatever it is, under the following form:

$$\frac{\partial S}{\partial t} = \sigma(x,y)\, \max\left[K_p\, \frac{|\bar{\nabla}S|}{p_{st}} \tanh\left[\frac{p_{st}}{|\bar{\nabla}S|}\right] , K_g\, \frac{\sigma(x,y)}{\sigma_1} \tanh\left[\frac{\sigma_1}{\sigma(x,y)}\right] \right] \tag{28}$$

This equation of evolution has a structure of partial differential equation except in some particular cases as constant initial profile and uniform environment. A large ratio $\frac{K_p}{K_g}$ will warranty the growth of a faceted crystal because the first argument of the function max will remain predominant even for a flat profile: the step propagation is thus much larger than the step generation. We consider this equation as powerful and the following examples show the present model can simulate stable or unstable growth in non-uniform environment, non-steady environment or anisotropic growth. Let us first verify the 1-D version of Eq.(28) leads to the same results as those obtained in Part.II.

The 1-D version of Eq.(28) is obviously:

$$\frac{\partial S}{\partial t} = \sigma(x) \max\left[K_p \frac{\frac{\partial S}{\partial x}}{p_{st}} \tanh\left[\frac{p_{st}}{\frac{\partial S}{\partial x}}\right], K_g \frac{\sigma(x)}{\sigma_1} \tanh\left[\frac{\sigma_1}{\sigma(x)}\right] \right] \qquad (29)$$

To show that Eq.(29) gives the same results than those obtained in the illustration in Part.II, we have to solve it with an equivalent constraint. In the previous computation we had fix the inter-step distance by controlling the step generation at x_0. For the present continuous problem, the PDE.(29), the equivalent constraint is a boundary condition of Neumann type at x_0. Then a straight-forward finite difference algorithm, keeping fixed the first derivative in x_0, gives results identical to the discrete problem solved in Part.II.

In this simulation we have chosen a large ratio $\frac{K_p}{K_g}$ in order to simulate the growth of a well faceted crystal: K_p, K_g, p_{st} and σ_1 are respectively equal to 2, 0.04, 1 and 0.1. The Fig.5 defines the integration domain and reminds us the supersaturation profile. On this figure d equals 0.75. The Neumann boundary condition at x=0 equals −1 in accordance with Part.II.

- Fig.6a and Fig.6b show the train profile and its first derivative obtained as steady state when the drop of supersaturation is only d=0.8. The latter curve corresponds to the step density. The density in the left part of the integration domain leads to an equivalent interstep distance of 2 which becomes 0.78 in the right part. Those values lead to two values of the function G whose ratio is 1.25 ; i.e. exactly the expected value.
- When d passes a critical value the growth can no longer be uniform and for d=0.75 we obtain the pattern described by Fig.7a and Fig.7b. Those figures correspond to the interface profile and its first derivative after an integration of 400 time units. And because $G(1)$=0.76 , this resolution is just at the border of the instability.

We are going now to present several examples obtained thanks to a 2-D integration of the surface kinetics as modelized by the present study.

A typical resolution of the 2-D problem, defined by Eq.(28), is illustrated on Fig.8. The initial conditions are defined on Fig.8a as a gaussian profile given to the function S at t=0. Then the integration is performed on the square $[-1,1]^2$ with an uniform supersaturation. The parameters are chosen as follows: K_p=1, p_{st}=1, K_g=0.02 and σ_1=0.1. At time t=0.4 Fig.8b shows the initial gaussian has spread provoking the growth of the whole face. At time t=0.8 most of the initial "steps" have already reached the boundaries of the square as shown by Fig.8c. At time t=4 Fig.8d indicates a flat face is regularly growing.

An other interesting illustration is the response to an unsteady environment. Suppose an inhomogeneous supersaturation of the form: $\sigma_I = exp(-x^2-y^2)$ is applied at the interface. After some time interval the integration gives a profile close to Fig.8a. At this instant we fix the supersaturation equal to $\sigma = 1-0.8\,\sigma_I$. Then 0.8 time unit later the profile becomes more complex as shown by Fig.9b. Creation points are still at the center of the square but new ones have appeared at the borders. At 0.8 time unit more, the generation centers at the boundary have overwhelmed the ones of the

beginning. At 4 time units after the change of supersaturation the growth is driven by 4 generation centers located at the corners of the square. The Fig.9c shows the corresponding pattern. Fig.9d finally presents the interface state after 4 additional time units.

Anisotropic growth can also be simulate by giving some advantage to preferred directions. This privilege is achieved in Eq.(25) when the normal fits with certain orientations. Then the step kinetic coefficient, K_p in Eq.(28), becomes a function of the gradient of S. The set of Fig.10 corresponds to the integration of Eq.(28) in an uniform environment and where K_p is non-vanishing only when the gradient fits with given orientations. Fig.10a and Fig.10b present the pattern with the favored directions $\pi/6$ and $-\pi/4$. The direction $\pi/6$ has a kinetic coefficient twice as the direction $-\pi/4$. Fig.10a shows some irregularities resulting from lack of numerical precision. There are damped after some time as illustrated by Fig.10b. This happens thanks to the nice mathematical properties of Eq.(28). Indeed, it can be easily shown the time integration of Eq.(28) with uniform σ leads to smoother and smoother profiles. Fig.10c shows a growth where the direction $3\pi/4$ is just one third more favored than direction $\pi/3$. Finally Fig.10d represents the pattern of the growth owing to three equally favored directions: $\pi/2$, $\pi/6$ and $-\pi/6$.

V.] Conclusion

We have presented a study about the coupling between Kinetics and Hydrodynamics related to the growth of faceted crystals. To well pose the problem we need a crystal kinetics depending on the supersaturation right along the crystal face, but not on the supersaturation in the bulk of the fluid. We have exposed a new model of generalized kinetics that is a direct consequence of the Burton-Cabrera-Frank model of step propagation. The result is provided under the form of a partial differential equation of which solution gives the interface profile. This equation allows the growth of faceted crystal in non-uniform environment and is also able to predict the morphological instability of a face.

Several examples of application, given in Part.IV, show it should be interesting to couple this interfacial kinetics with the large system of PDE governing the transport in the fluid phase. This is the final point of the present study and the above mentioned huge coupling is the logical continuation of this work. The procedure articulates as follows. The resolution of Eq.(28), if σ is known, allows to evaluate the growth rate; i.e. $\frac{\partial S}{\partial n}$, the normal derivative of the supersaturation at the interface. This quantity is a relevant boundary condition to solve Eq.(10). Thus one obtains the complete field of supersaturation, including at the interface. The latter allows to integrate Eq.(28), and so on. In case of fluid motion this cycle must include the resolution of Eq.(9).

On the way to this new model we have revisited an other consequence of the Burton-Cabrera-Frank model: the criterion of Kuroda, Irisawa and Ookawa for the stability of a growing interface in non-uniform environment. We have shown this criterion is valid for any train as soon as the latter contains a ten of steps. Moreover this criterion furnishes an immediate explanation for the destabilizing role of a large growth rate. As for the role played by the size of the crystal face, we have applied the previous criterion to the coupling with two typical fluid flows. Several restricting consequences of the BCF model are thus proposed to experimental validation.

Acknowledgements

The author would like to thank Blaise Simon and Edith Bourret for helpful discussions and encouragements. This work was supported by the International Exchange Program CNRS/NSF.

References

[1] D. Elwell and H.J Scheel, *Crystal Growth from High-Temperature Solutions,* (Academic Press, London, 1975)

[2] W.R. Wilcox, *J. Crystal Growth* 65 (1983) p. 133

[3] A.A. Chernov, *Modern Crystallography III: Crystal Growth,* (Springer-Verlag, Berlin, 1984)

[4] G.H. Gilmer, R. Ghez and N. Cabrera, *J. Crystal Growth* 8 (1971) p. 79

[5] A.A. Chernov, *Sov. Phys. Usp.* 4 (1961) p. 129

[6] W.K. Burton, N. Cabrera and F.C. Frank, *Phil. Trans. Roy. Soc. London,* A 243 (1951) p. 299

[7] T.Kuroda, T.Irisawa and A. Ookawa *J. Crystal Growth,* 42 (1977) p. 41

[8] P. Bennema, in *Crystal Growth,* Ed. H.S. Peiser (pergamon, Oxford, 1967) p. 413

[9] S. Zerfoss and S.I. Slawson, *Am. Mineralogist,* 41, (1956) p. 598

[10] A. Carlson, in: *Growth and Perfection of Crystals,* Eds. R.H. Doremus, B.W. Roberts and D. Turnbull, (Wiley, New York, 1958) p. 421

[11] R. Janssen-Van Rosmalen and P. Bennema, *J. Crystal Growth,* 42 (1977) p. 224

[12] C. Kumar, J. Estrin and G.R. Youngquist, *J. Crystal Growth,* 54 (1981) p. 176

[13] B. Simon, J.M. Cherel and P. Haldenwang, Submitted.

[14] C. Kumar and J. Estrin, *J. Crystal Growth,* 51 (1981) p. 323

[15] G.K. Batchelor, *An Introduction to Fluid Dynamics,* (Cambridge University Press, 1967)

[16] A. Bejan, *Convection Heat Transfer,* (Wiley, New York, 1984)

[17] L.M. Milne-Thomson, *Theoretical Hydrodynamics,* (Mac Millan, New York, 1968)

[18] F. Rosenberger, *Fundamentals of Crystal Growth I,* (Springer-Verlag, Berlin, 1979)

[19] G. Muller and G. Neumann, *J. Crystal Growth,* 63 (1983) p. 58

Figure Captions

Fig.1: Plot of $G(z)=z^{-1}tanh(z)$

Fig.2: Typical profile of supersaturation imposed to a short train of step (discrete problem)

Fig.3: a) Steady surface profile of a crystal growing stably in an imposed supersaturation drop d=0.20 (discrete problem) ; b) corresponding step density profile.

Fig.4: a) Instantaneous surface profile of a crystal surface subject to a morphological instability resulting from a supersaturation drop d=0.25 (discrete problem) ; b) Corresponding instantaneous step density profile.

Fig.5: Typical profile of supersaturation imposed to integration of Eq.(29) (continuous problem)

Fig.6: a) Steady surface profile of a crystal growing stably in an imposed supersaturation drop d=0.20 (continuous problem) ; b) corresponding step density profile.

Fig.7: a) Instantaneous surface profile of a crystal surface subject to a morphological instability resulting from a supersaturation drop d=0.25 (continuous problem) ; b) Corresponding instantaneous step density profile.

Fig.8: Surface profiles (seen from above) furnished by the level curves of function S. the crystal grows according to Eq.(29) in an uniform environment ; a) initial profile ; b) at time=0.4 ; c) at time=0.8 ; d) at time=4.

Fig.9: Surface profiles of a crystal growing in an unsteady environment ; a) at 0.8 time units after the change of supersaturation distribution. the maximum is now at the corners ; b) at 0.8 time units later ; c) at time=4 ; d) at time=8.

Fig.10: Anisotropic growth. (the reduced kinetics are given in parentheses) ; a) and b) favored directions: $\pi/6$ (2) and $-pi/4$ (1) ; c) favored directions: $3\pi/4$ (2) and $\pi/3$ (1.5) ; d) favored directions: $\pi/2$ (1), $\pi/6$ (1) and $-\pi/6$ (1)

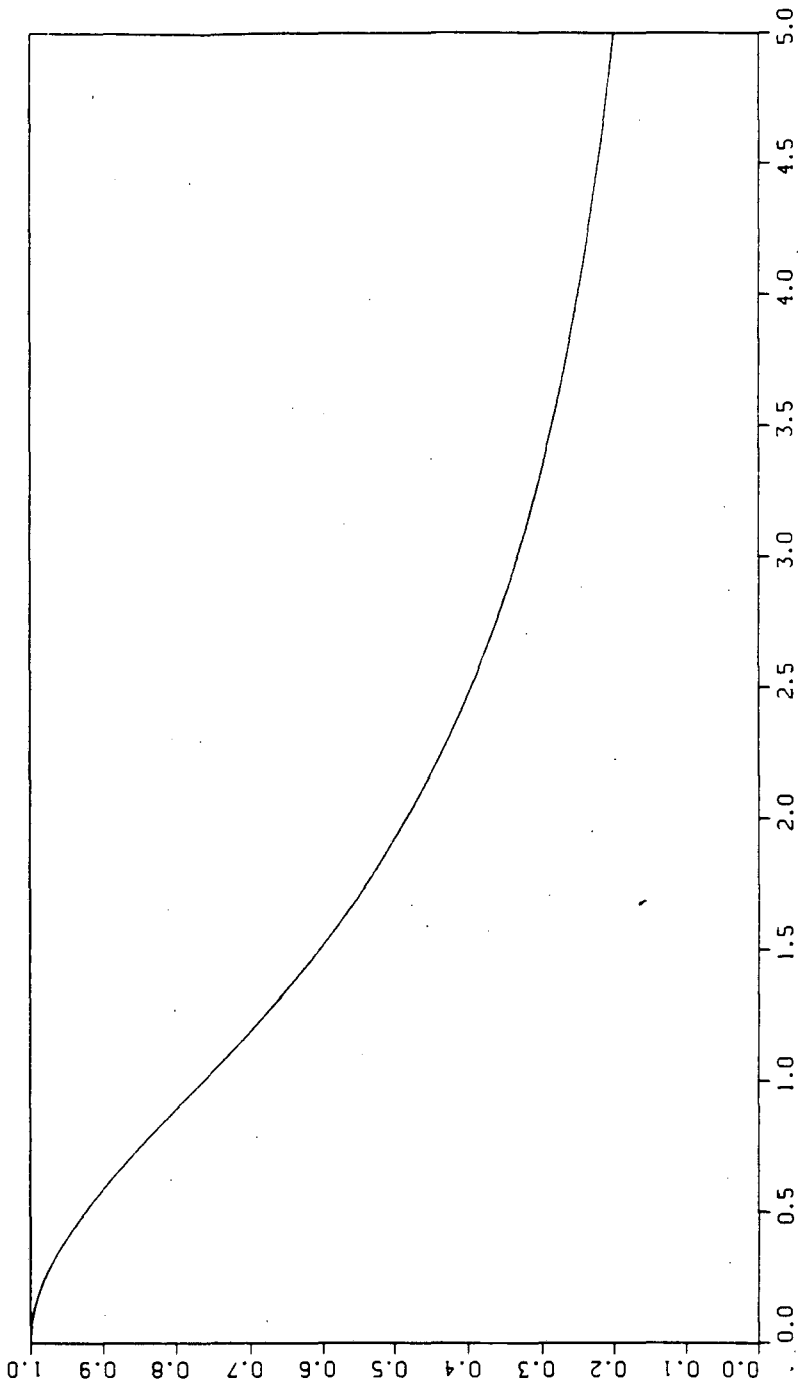

Fig.1

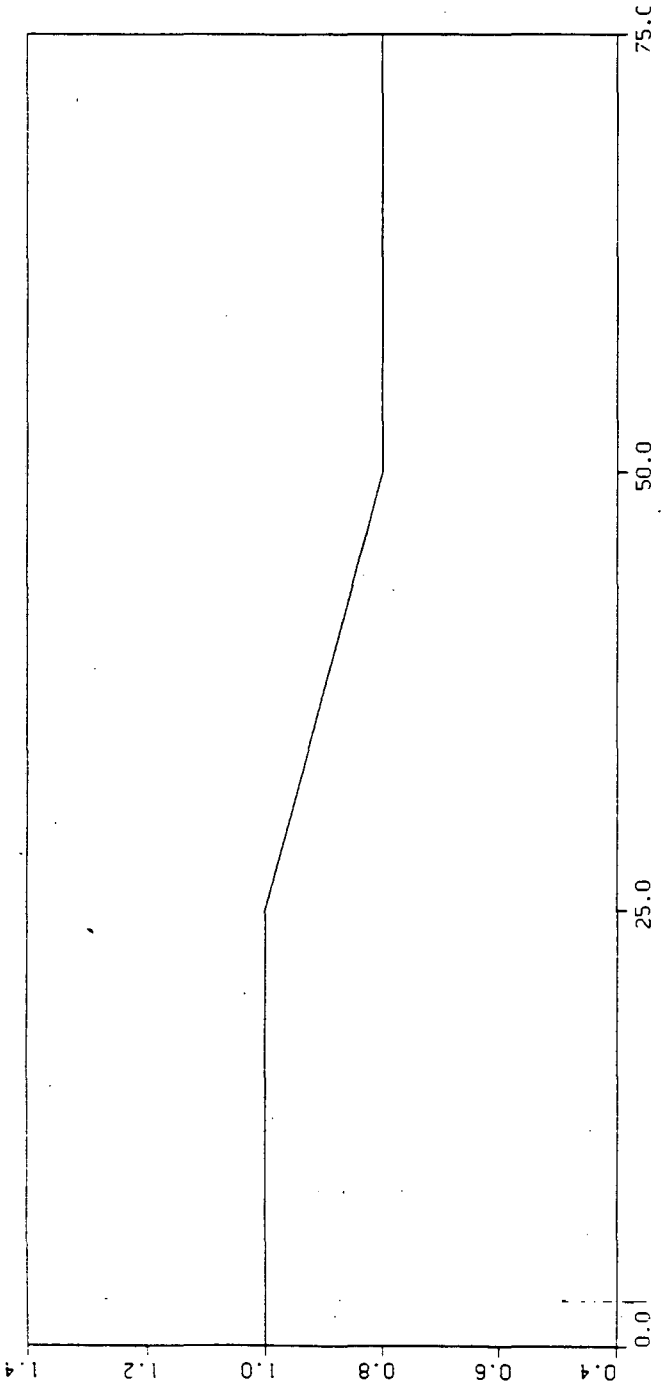

Fig.2

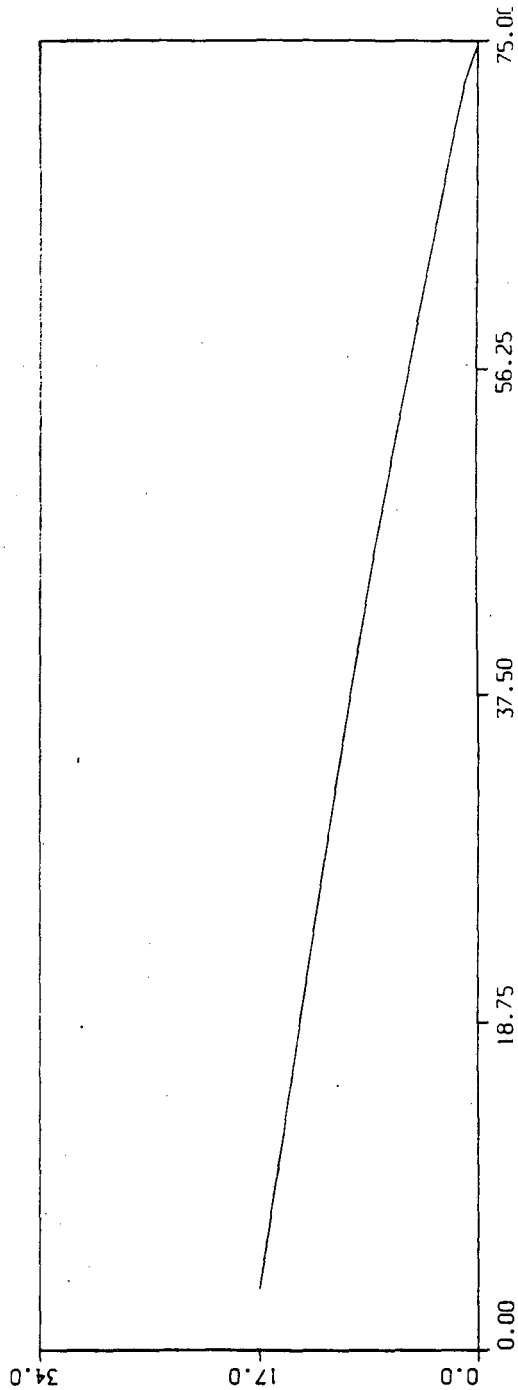

Fig.3a

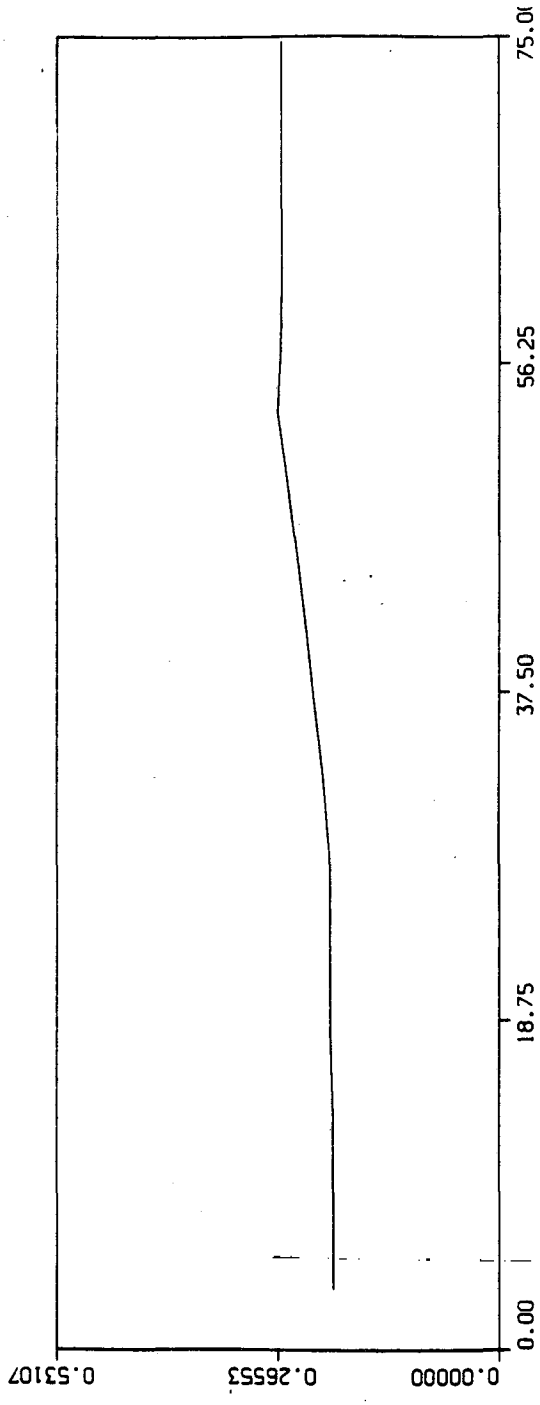

Fig.3b

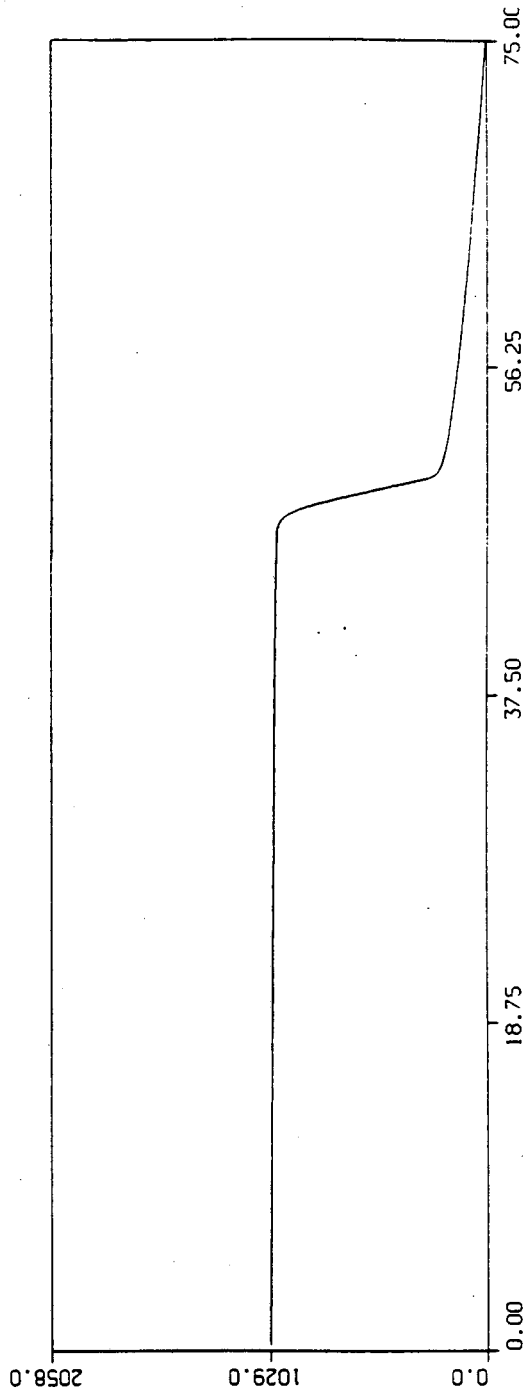

Fig.4a

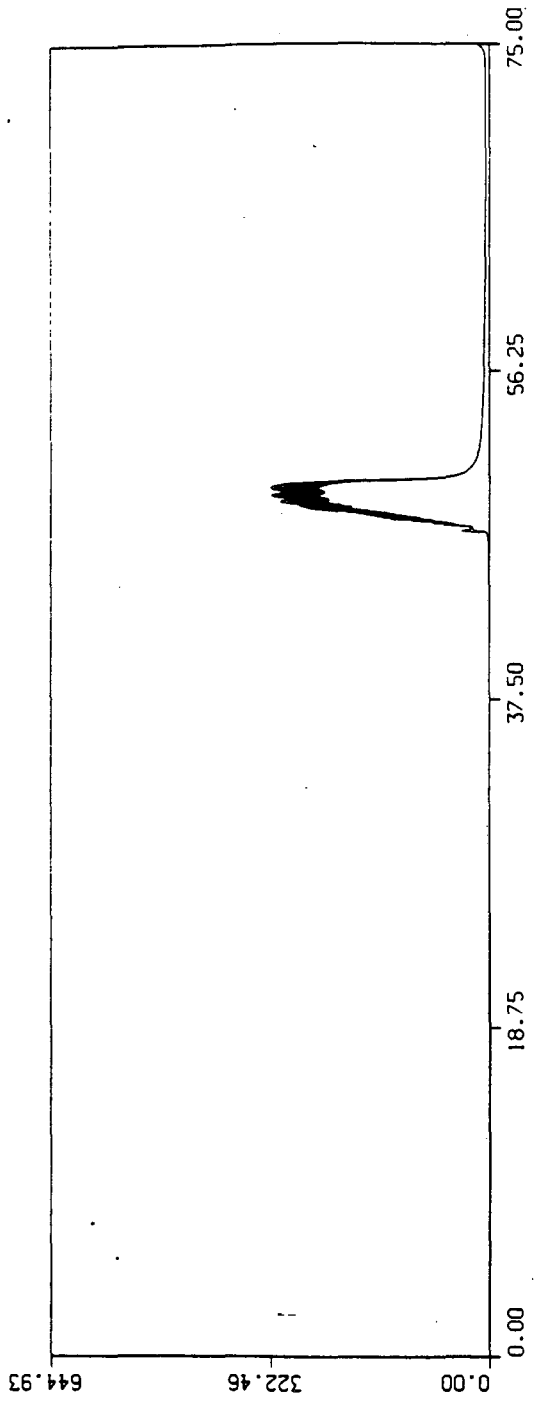

Fig.4b

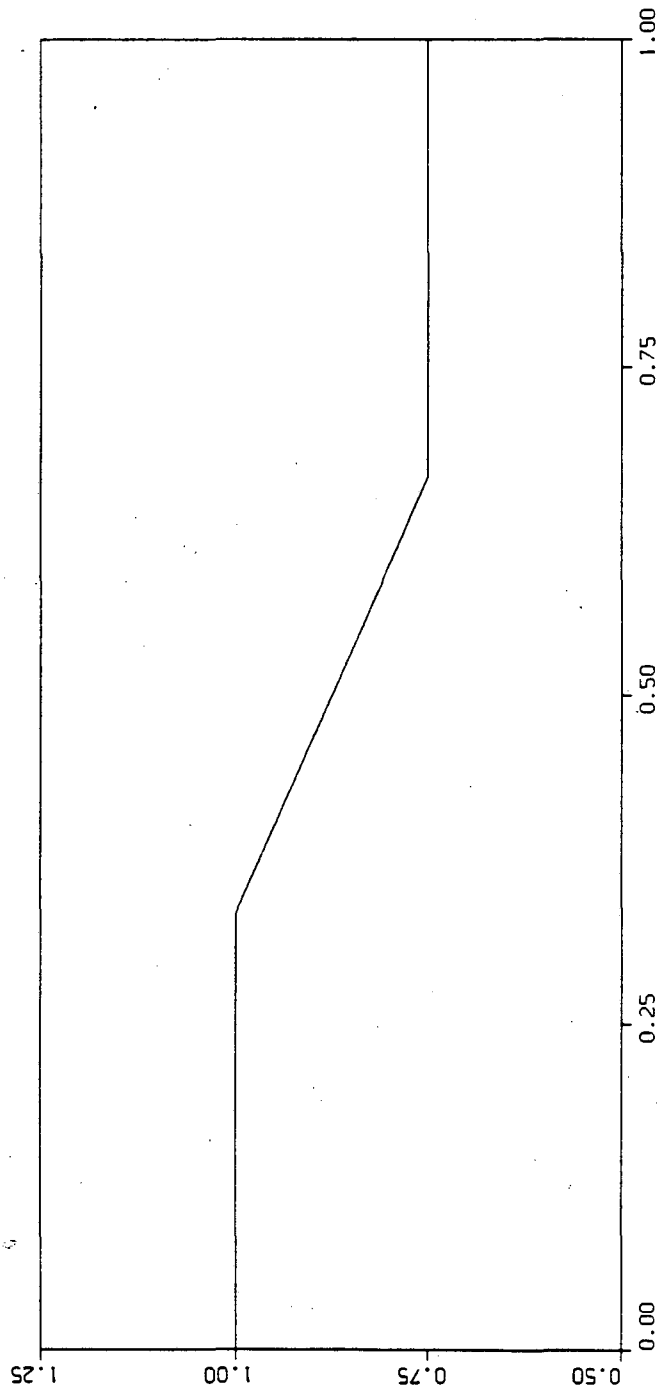

Fig.5

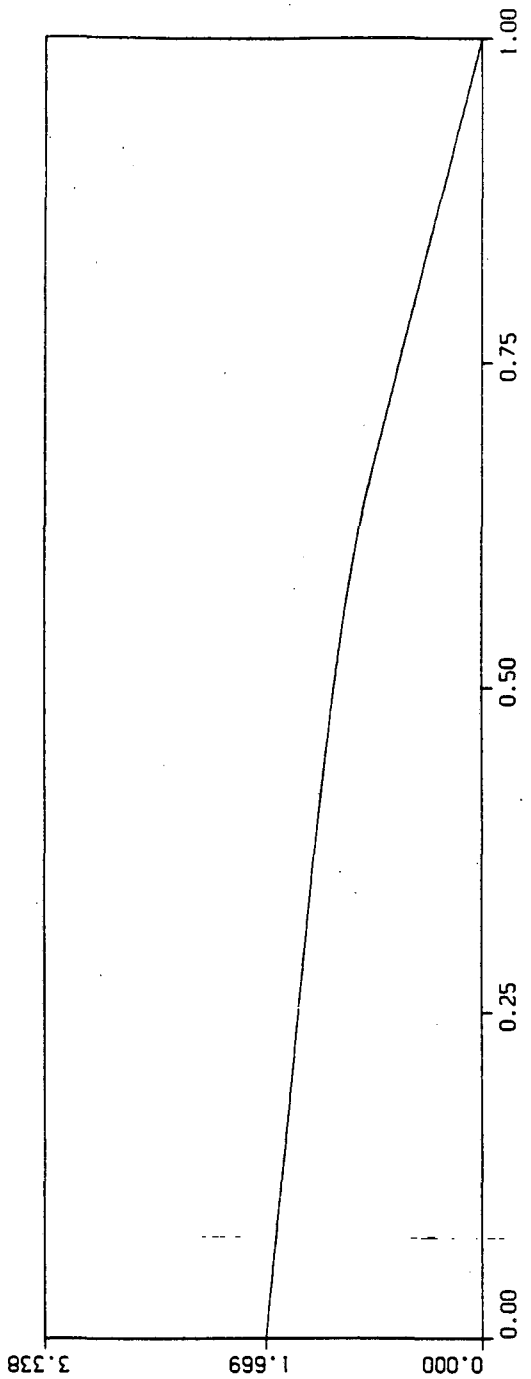

Fig.6a

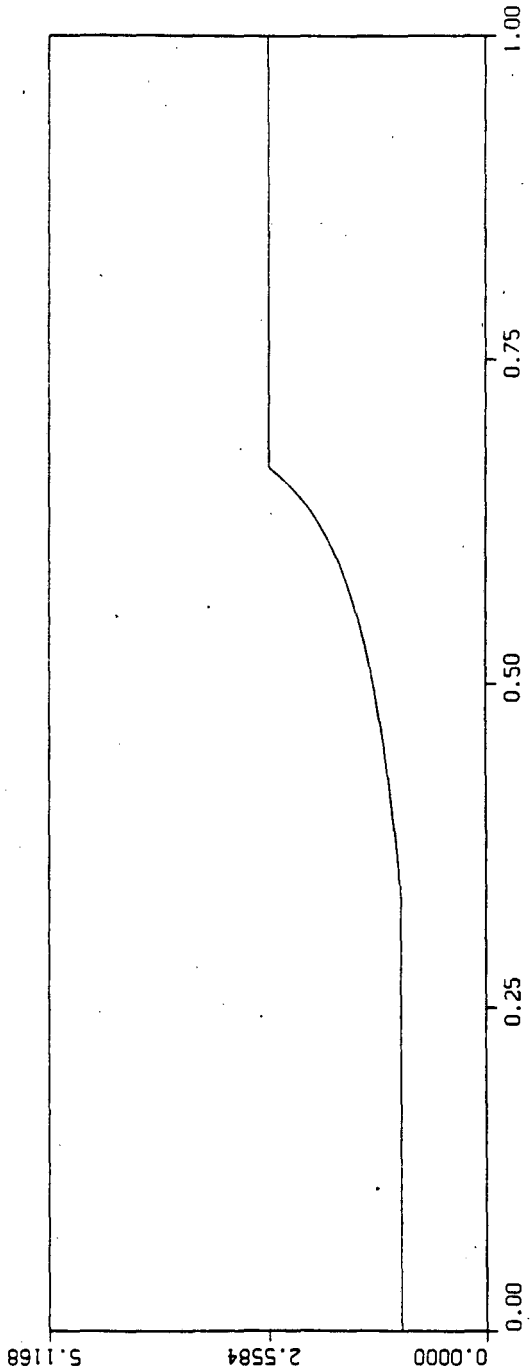

Fig.6b

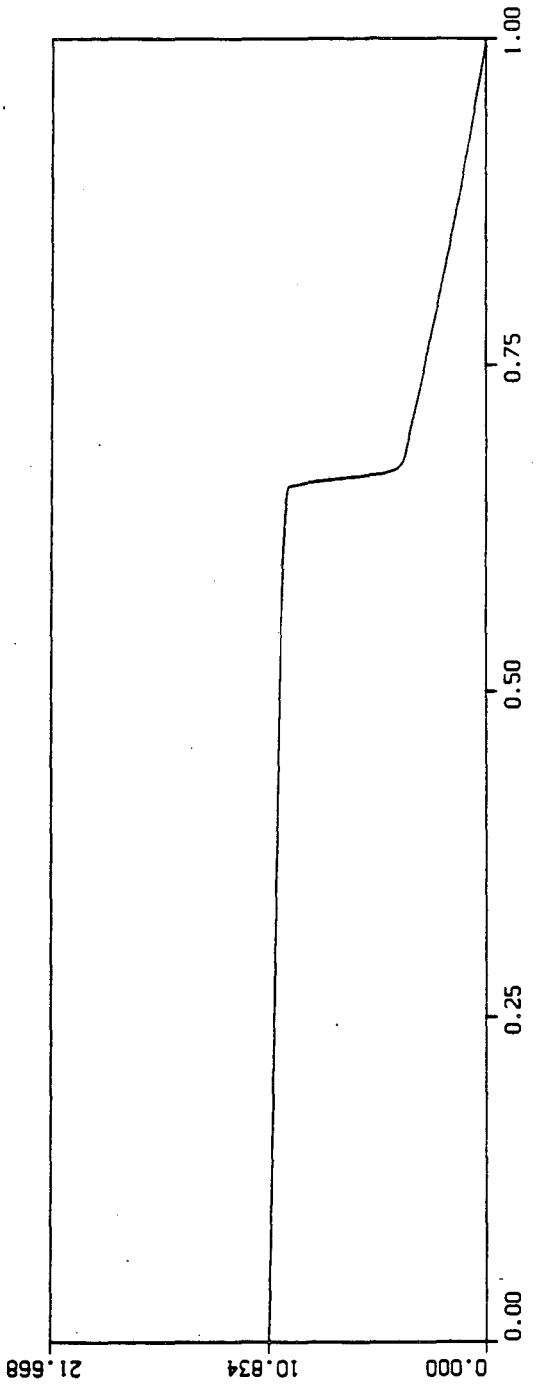

Fig.7a

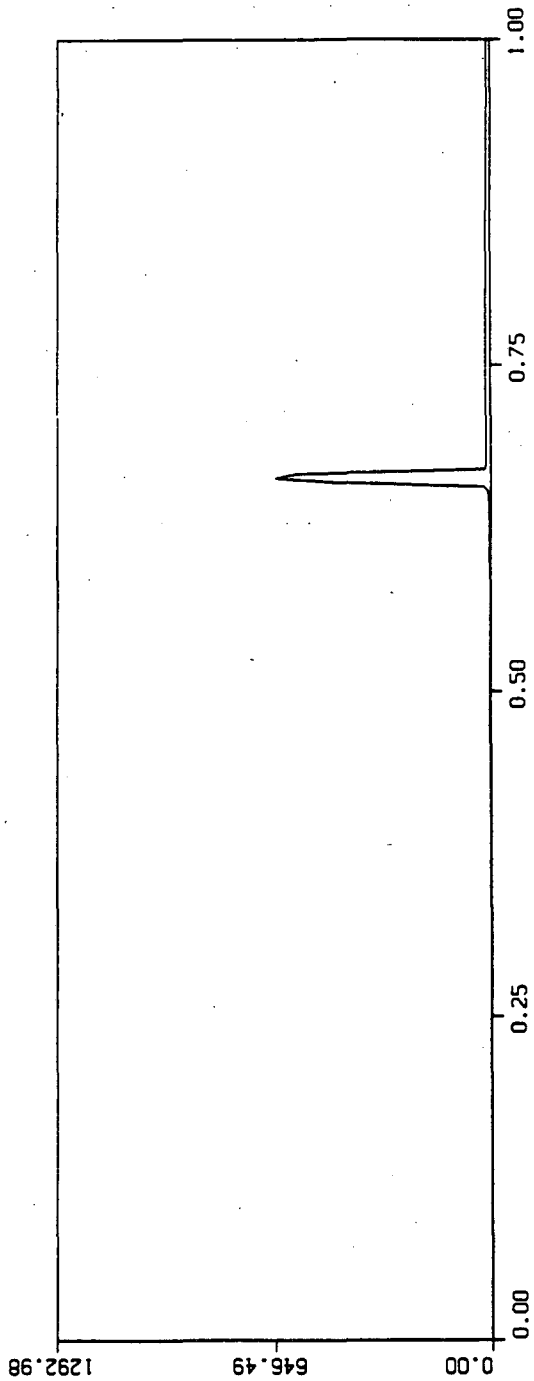

Fig.7b

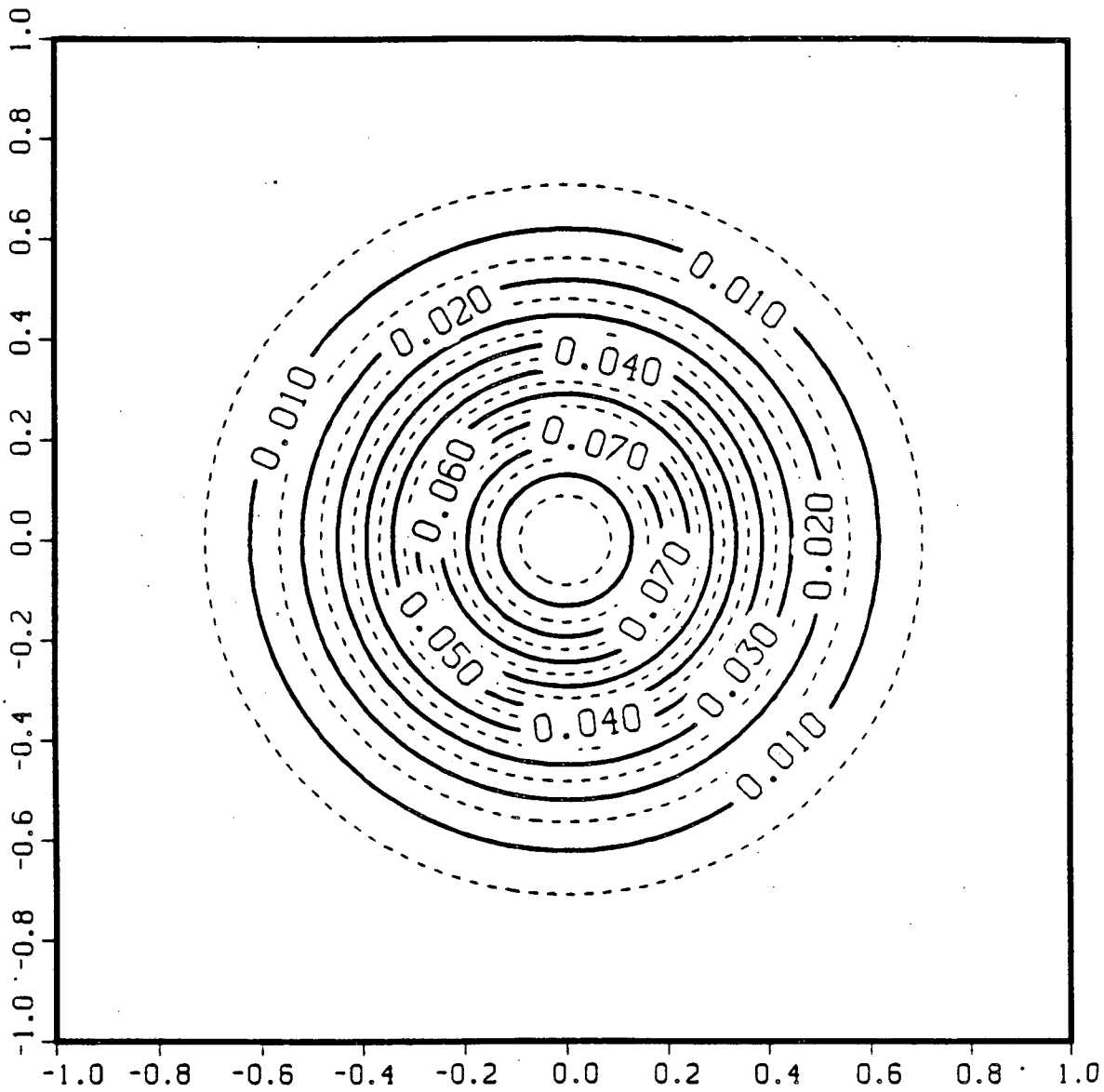
1.0
0.8
0.6
0.4
0.2
0.0
-0.2
-0.4
-0.6
-0.8
-1.0
-1.0 -0.8 -0.6 -0.4 -0.2 0.0 0.2 0.4 0.6 0.8 1.0
0.010
0.020
0.040
0.070
0.060
0.050
0.030

Fig.8a

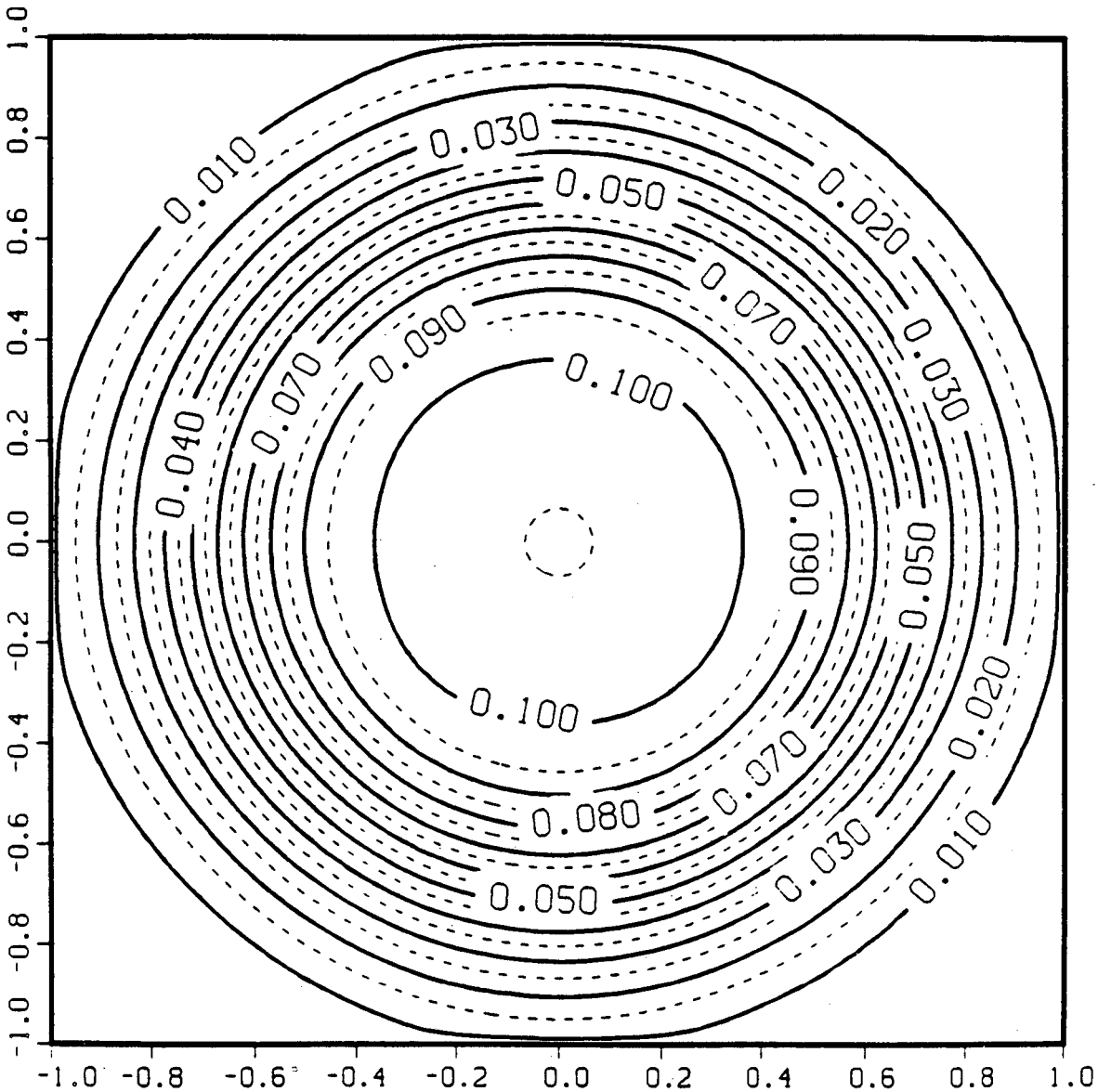
0.010
0.030
0.050
0.020
0.070
0.030
0.090
0.050
0.070
0.040
0.100
0.060
0.090
0.050
0.100
0.070
0.080
0.020
0.030
0.050
0.010
1.0
0.8
0.6
0.4
0.2
0.0
-0.2
-0.4
-0.6
-0.8
-1.0
-1.0 -0.8 -0.6 -0.4 -0.2 0.0 0.2 0.4 0.6 0.8 1.0

Fig.8b

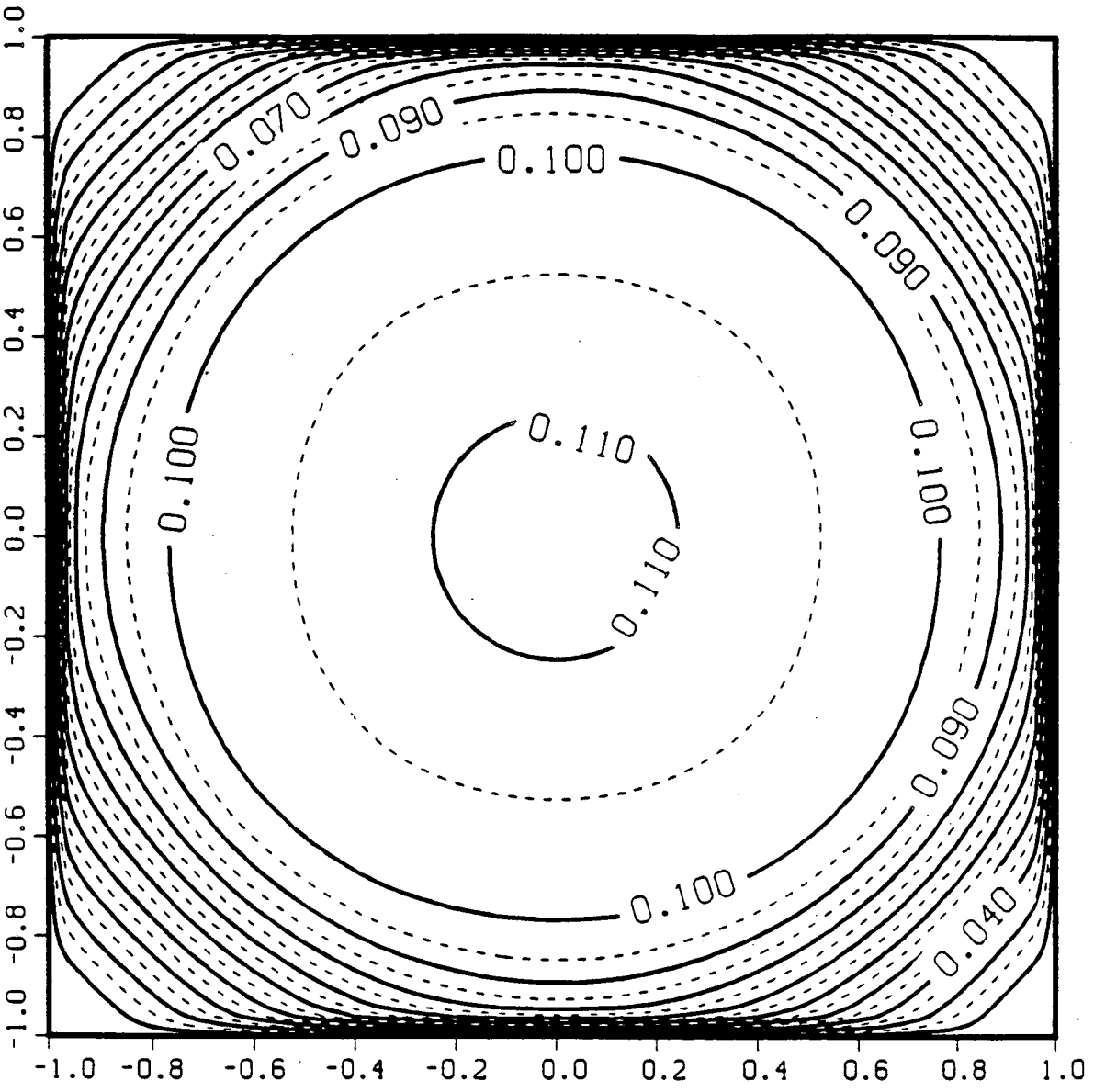
0.070
0.090
0.100
0.090
0.100
0.110
0.110
0.100
0.090
0.100
0.040
1.0
0.8
0.6
0.4
0.2
0.0
-0.2
-0.4
-0.6
-0.8
-1.0
-1.0 -0.8 -0.6 -0.4 -0.2 0.0 0.2 0.4 0.6 0.8 1.0

Fig.8c

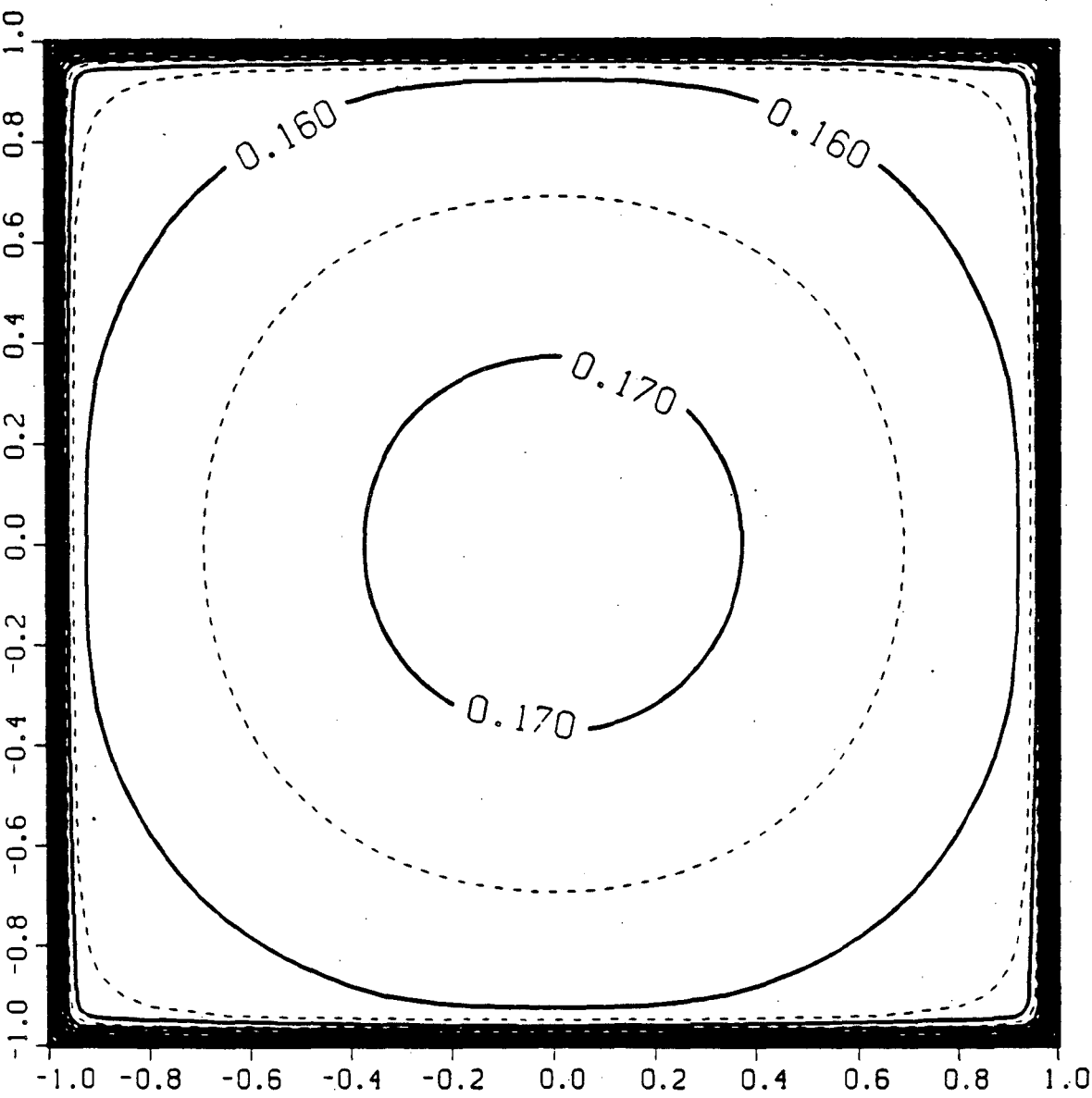
0.160
0.160
0.170
0.170
1.0
0.8
0.6
0.4
0.2
0.0
-0.2
-0.4
-0.6
-0.8
-1.0
-1.0 -0.8 -0.6 -0.4 -0.2 0.0 0.2 0.4 0.6 0.8 1.0

Fig.8d

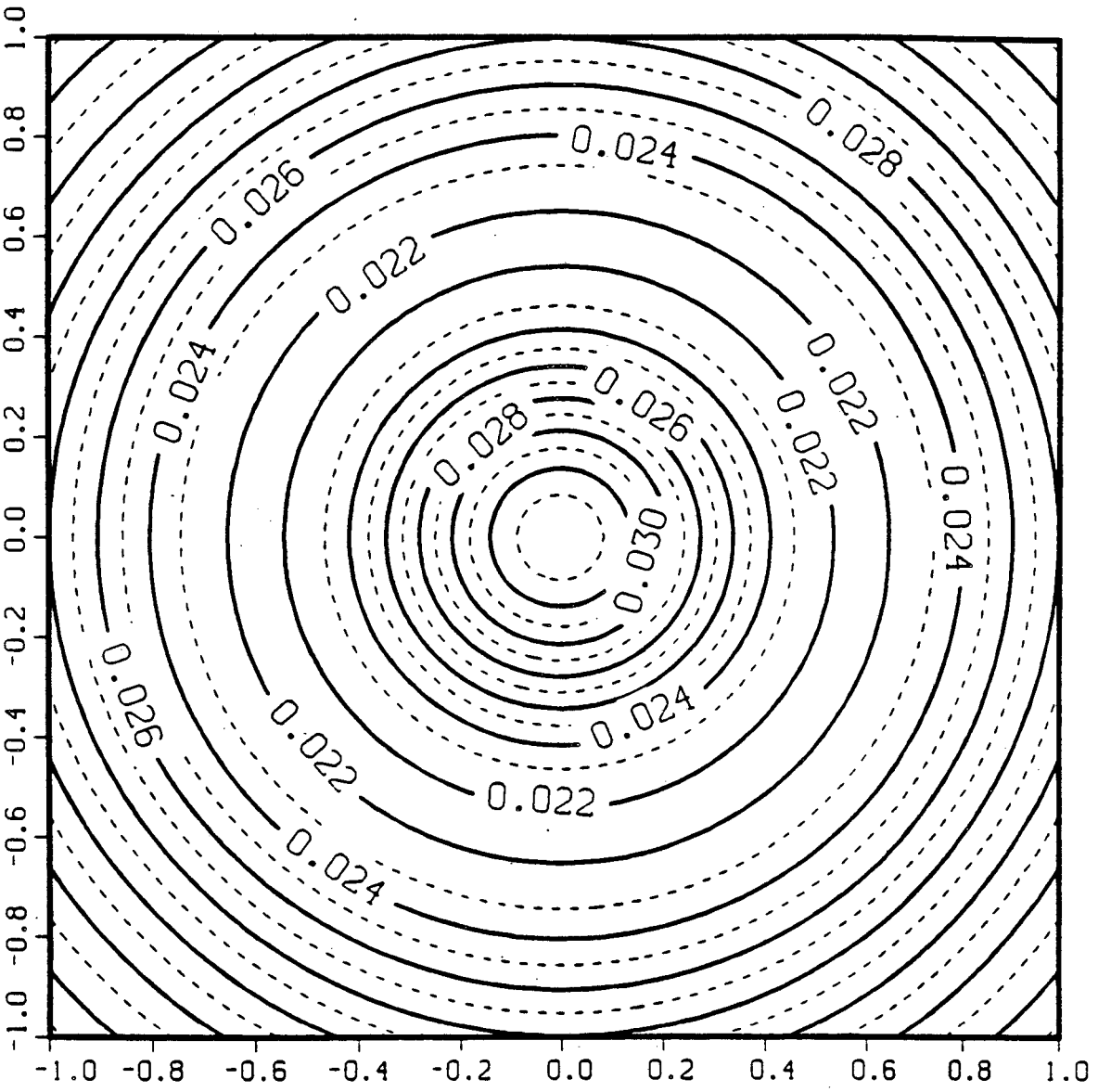
0.028
0.024
0.026
0.022
0.024
0.022
0.028
0.026
0.030
0.022
0.024
0.024
0.026
0.022
0.024
1.0
0.8
0.6
0.4
0.2
0.0
-0.2
-0.4
-0.6
-0.8
-1.0
-1.0 -0.8 -0.6 -0.4 -0.2 0.0 0.2 0.4 0.6 0.8 1.0

Fig.9a

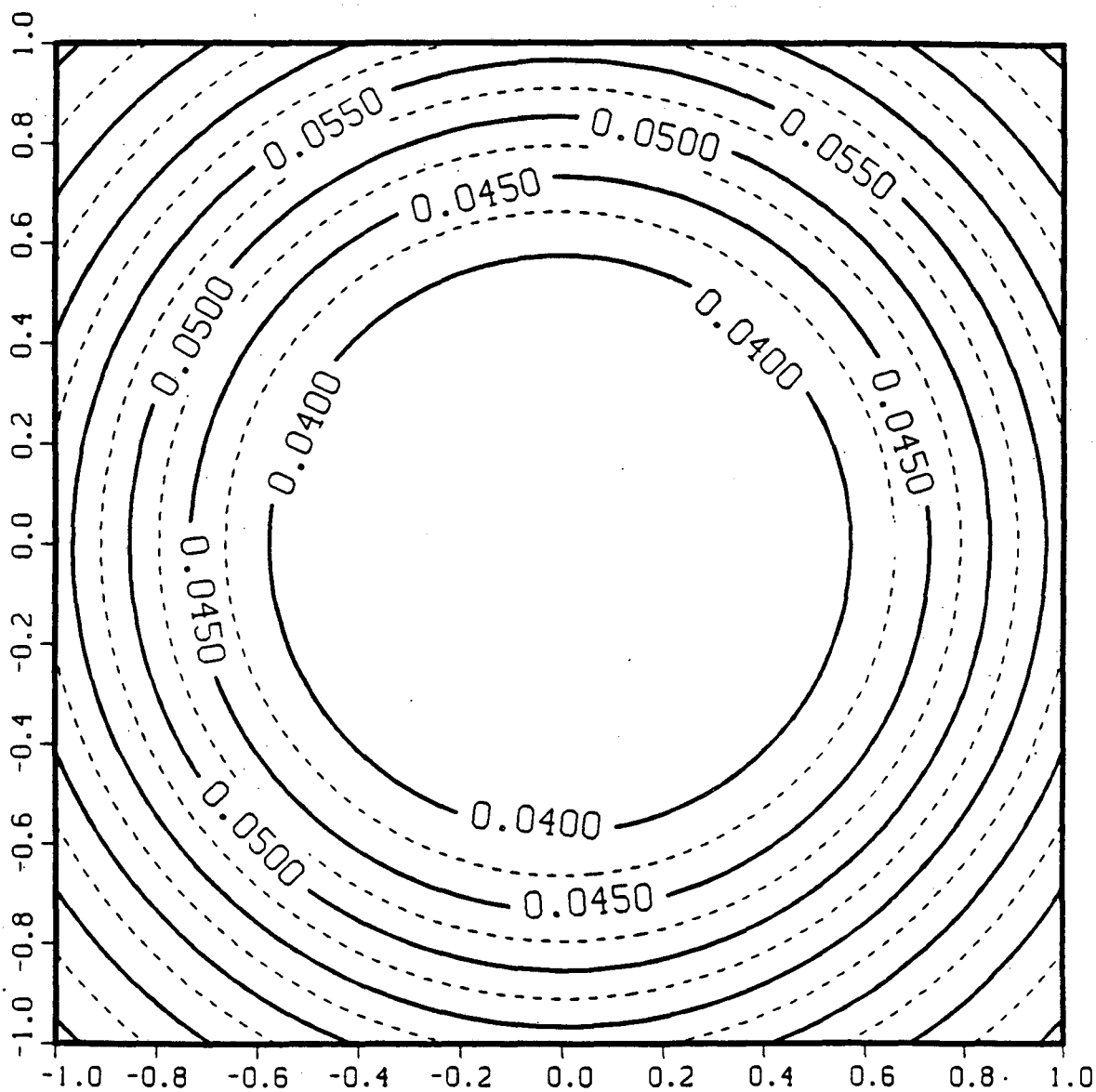
0.0550
0.0500
0.0450
0.0400
0.0400
0.0450
0.0500
0.0550
0.0500
0.0450
0.0400
0.0450
0.0500
1.0
0.8
0.6
0.4
0.2
0.0
-0.2
-0.4
-0.6
-0.8
-1.0
-1.0 -0.8 -0.6 -0.4 -0.2 0.0 0.2 0.4 0.6 0.8 1.0

Fig.9b

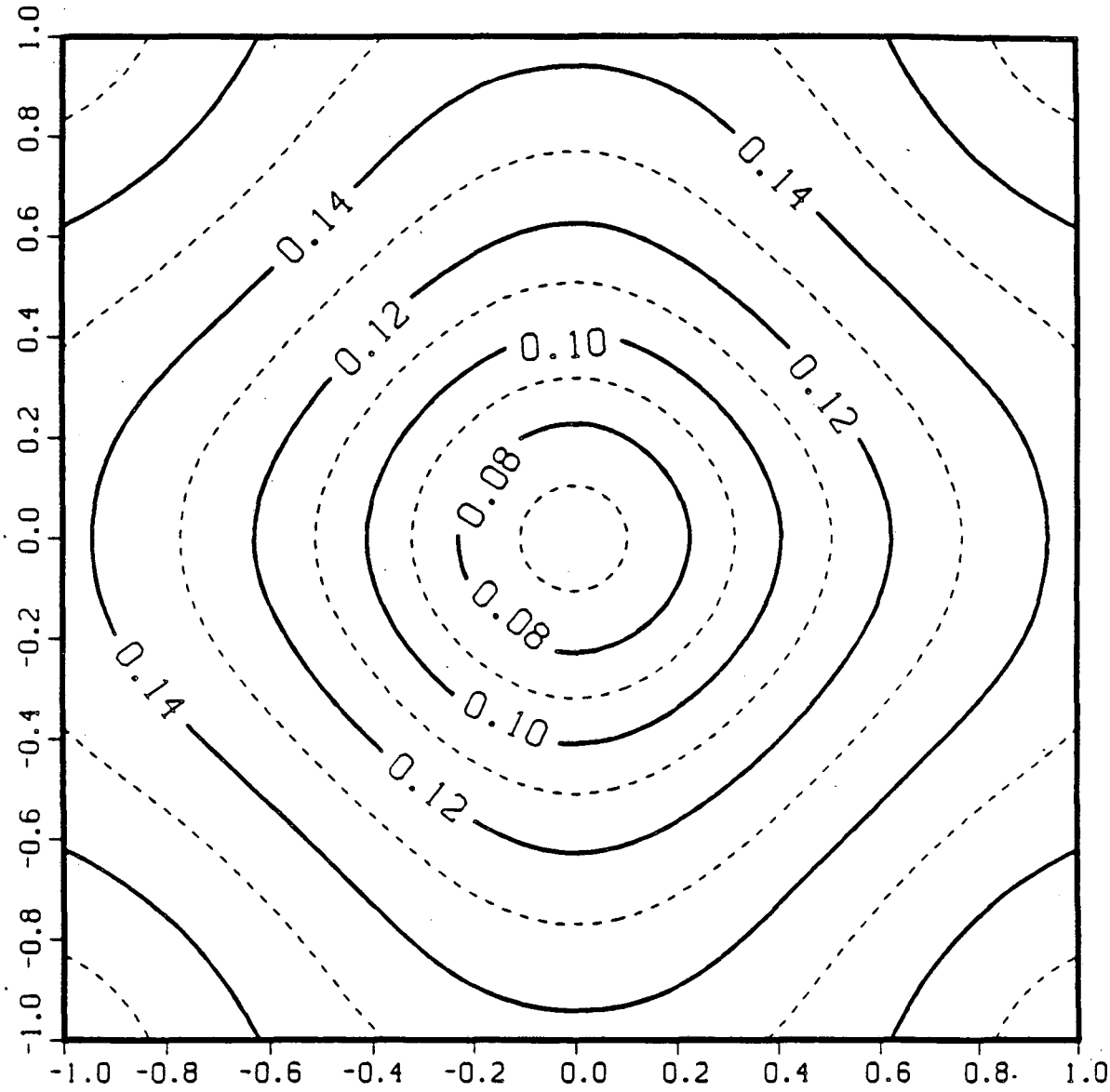
0.14
0.14
0.12
0.10
0.12
0.08
0.08
0.14
0.10
0.12
1.0
0.8
0.6
0.4
0.2
0.0
-0.2
-0.4
-0.6
-0.8
-1.0
-1.0 -0.8 -0.6 -0.4 -0.2 0.0 0.2 0.4 0.6 0.8 1.0

Fig.9c

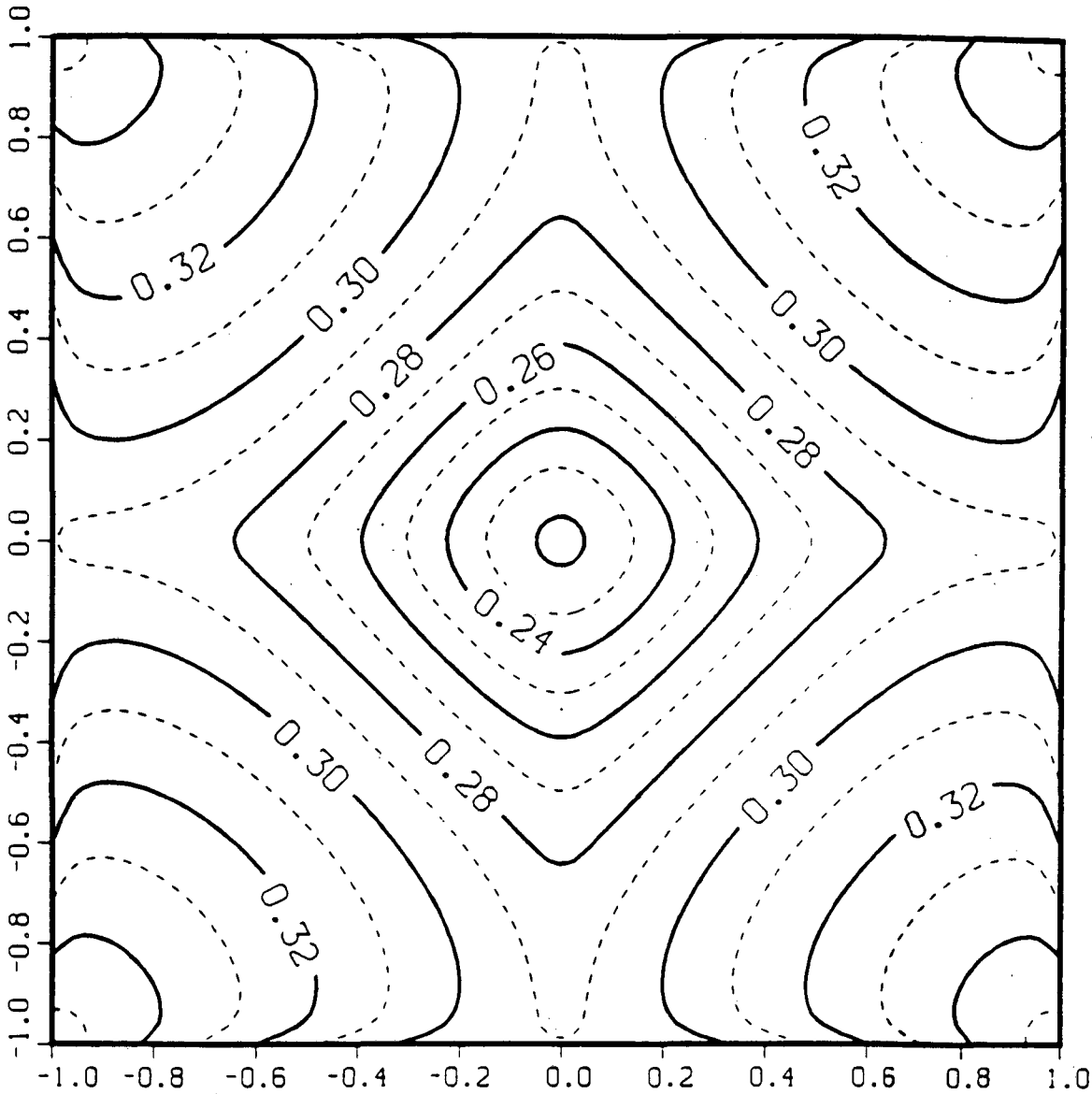

Fig.9d

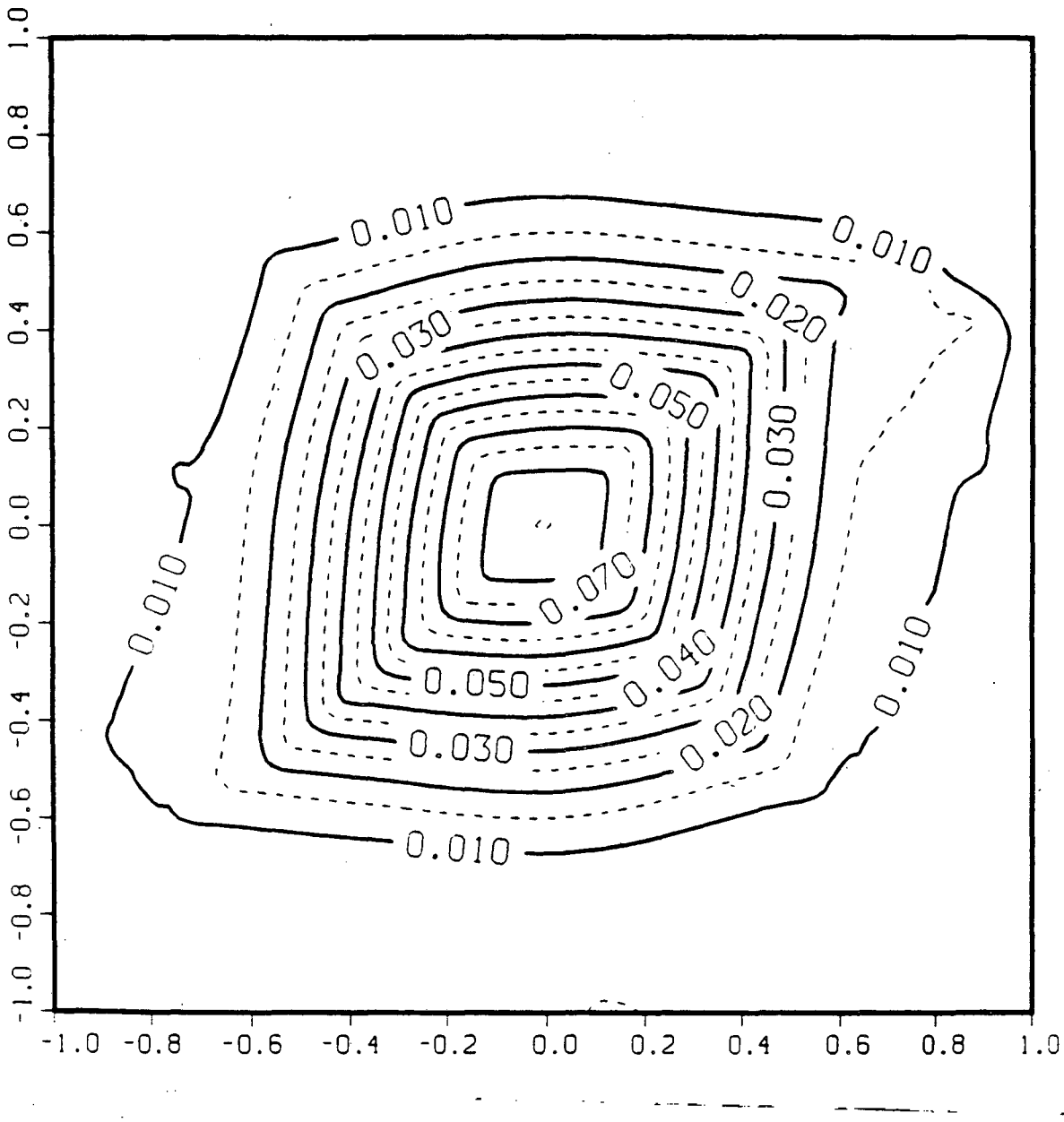
0.010
0.010
0.020
0.030
0.050
0.030
0.070
0.040
0.050
0.020
0.030
0.010
0.010
0.010
1.0
0.8
0.6
0.4
0.2
0.0
-0.2
-0.4
-0.6
-0.8
-1.0
-1.0 -0.8 -0.6 -0.4 -0.2 0.0 0.2 0.4 0.6 0.8 1.0

Fig.10a

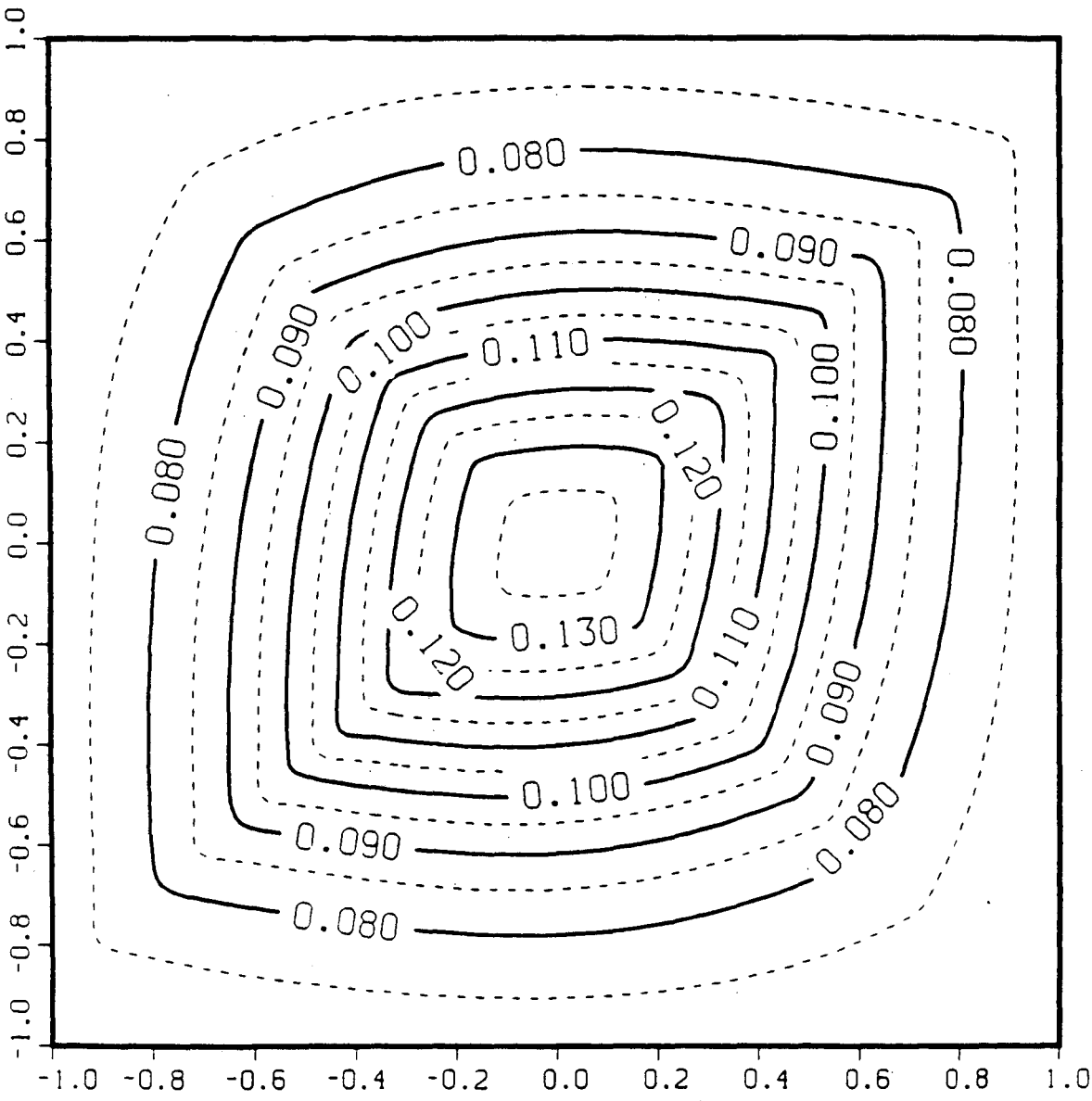
0.080
0.090
0.100
0.110
0.120
0.130
1.0
0.8
0.6
0.4
0.2
0.0
-0.2
-0.4
-0.6
-0.8
-1.0
-1.0 -0.8 -0.6 -0.4 -0.2 0.0 0.2 0.4 0.6 0.8 1.0

Fig.10b

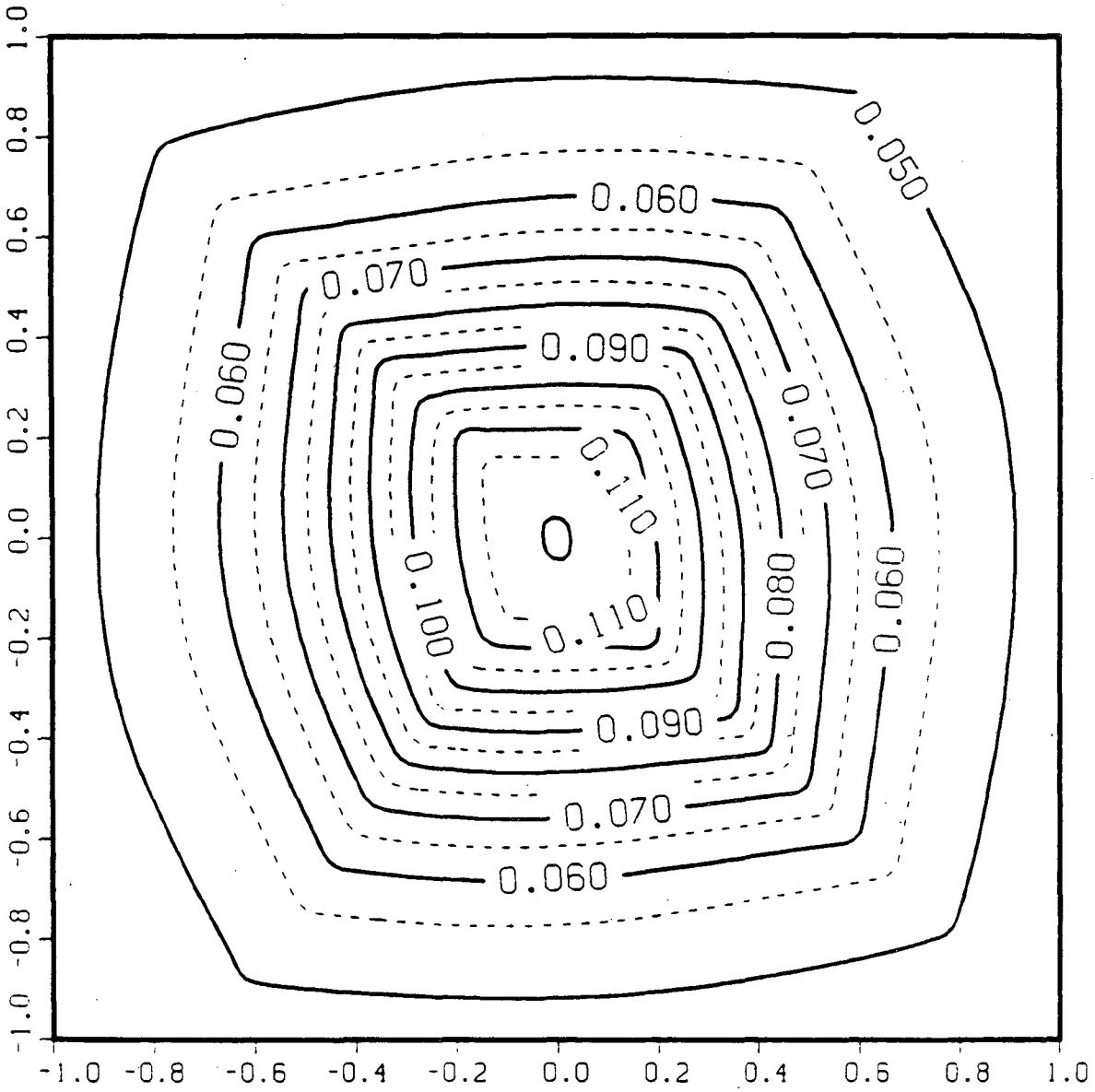
0.050
0.060
0.070
0.090
0.110
0
0.110
0.090
0.070
0.060
0.060
0.070
0.080
0.100
1.0
0.8
0.6
0.4
0.2
0.0
-0.2
-0.4
-0.6
-0.8
-1.0
-1.0 -0.8 -0.6 -0.4 -0.2 0.0 0.2 0.4 0.6 0.8 1.0

Fig.10c

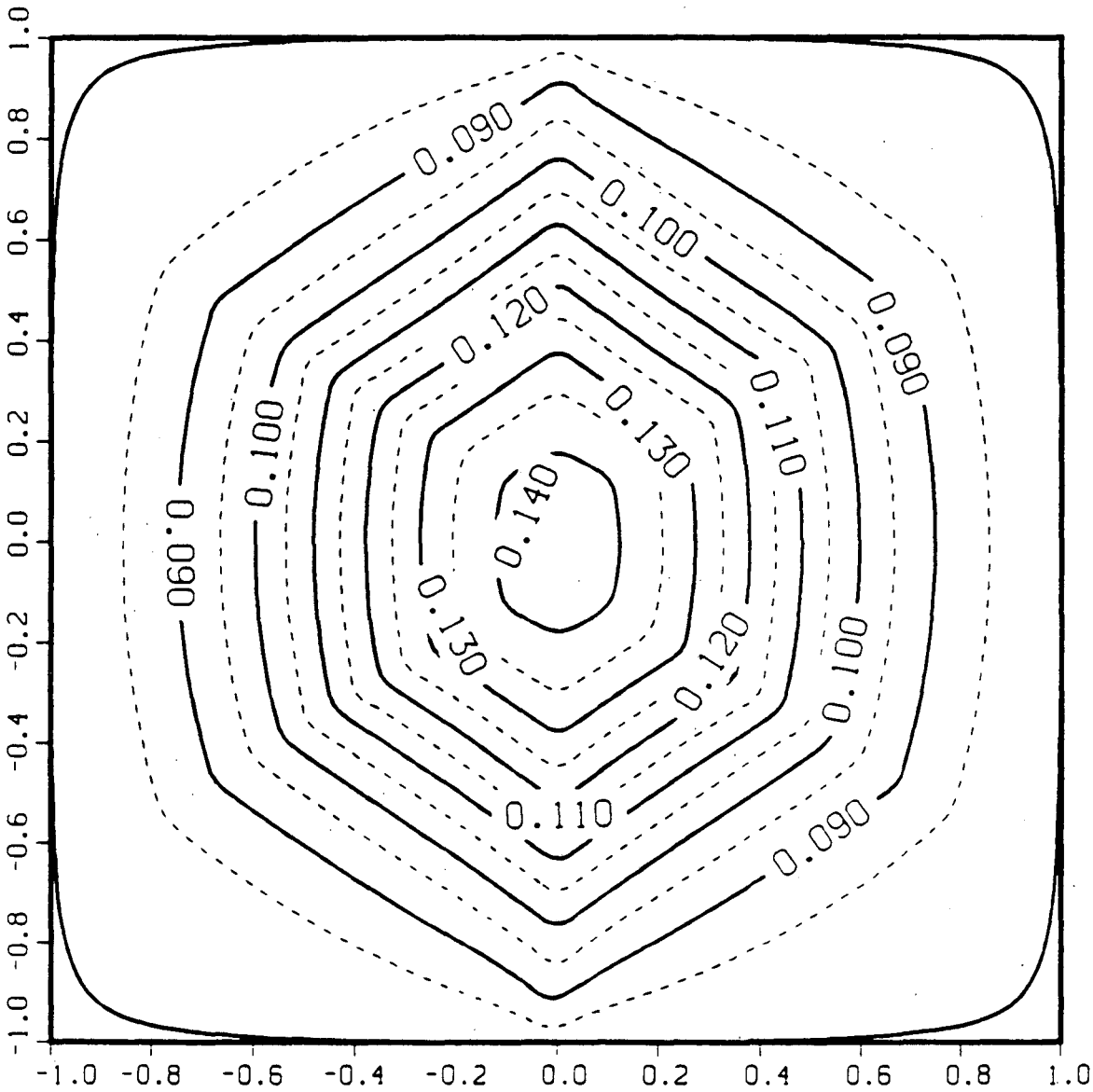
0.090
0.100
0.120
0.130
0.140
0.110
0.090
0.100
0.120
0.130
0.110
0.100
0.090
0.060
1.0
0.8
0.6
0.4
0.2
0.0
-0.2
-0.4
-0.6
-0.8
-1.0
-1.0 -0.8 -0.6 -0.4 -0.2 0.0 0.2 0.4 0.6 0.8 1.0

Fig.10d

LAWRENCE BERKELEY LABORATORY
TECHNICAL INFORMATION DEPARTMENT
UNIVERSITY OF CALIFORNIA
BERKELEY, CALIFORNIA 94720